

Alma Mater Studiorum Università di Bologna
Archivio istituzionale della ricerca

Seismic assessment of interacting structural units in complex historic masonry constructions by nonlinear static analyses

This is the final peer-reviewed author's accepted manuscript (postprint) of the following publication:

Published Version:

Degli Abbati, S., D'Altri, A.M., Ottonelli, D., Castellazzi, G., Cattari, S., de Miranda, S., et al. (2019). Seismic assessment of interacting structural units in complex historic masonry constructions by nonlinear static analyses. *COMPUTERS & STRUCTURES*, 213, 51-71 [10.1016/j.compstruc.2018.12.001].

Availability:

This version is available at: <https://hdl.handle.net/11585/691411> since: 2020-04-08

Published:

DOI: <http://doi.org/10.1016/j.compstruc.2018.12.001>

Terms of use:

Some rights reserved. The terms and conditions for the reuse of this version of the manuscript are specified in the publishing policy. For all terms of use and more information see the publisher's website.

This item was downloaded from IRIS Università di Bologna (<https://cris.unibo.it/>).
When citing, please refer to the published version.

(Article begins on next page)

This is the final peer-reviewed accepted manuscript of:

Stefania Degli Abbati, Antonio Maria D'Altri, Daria Ottonelli, Giovanni Castellazzi, Serena Cattari, Stefano de Miranda, Sergio Lagomarsino, *Seismic assessment of interacting structural units in complex historic masonry constructions by nonlinear static analyses*, Computers & Structures, Volume 213, 2019, Pages 51-71

ISSN 0045-7949

The final published version is available online at:
<https://doi.org/10.1016/j.compstruc.2018.12.001>

© 2018. This manuscript version is made available under the Creative Commons Attribution-NonCommercial-NoDerivs (CC BY-NC-ND) 4.0 International License

(<http://creativecommons.org/licenses/by-nc-nd/4.0/>)

Seismic assessment of interacting structural units in complex historic masonry constructions by nonlinear static analyses

Stefania Degli Abbatì¹, Antonio Maria D'Altri², Daria Ottonelli¹, Giovanni Castellazzi^{2*}, Serena Cattari¹, Stefano de Miranda², Sergio Lagomarsino¹

¹ DICCA, Dept. of Civil, Chemical Environmental Engineering, University of Genova Via Montallegro 1, Genova 16145, Italy

E-mail: stefania.degliabbati@unige.it, daria.ottonelli@unige.it, serena.cattari@unige.it, sergio.lagomarsino@unige.it

² DICAM, Dept. of Civil, Chemical, Environmental and Materials Engineering, University of Bologna Viale del Risorgimento 2, Bologna 40136, Italy

E-mail: antoniomaria.daltri2@unibo.it, giovanni.castellazzi@unibo.it, stefano.demiranda@unibo.it

*corresponding author: giovanni.castellazzi@unibo.it

ABSTRACT

The damage occurred due to past earthquakes highlighted that the seismic behavior of historic masonry structures characterized by an aggregation of units with an own seismic behavior (e.g. palaces, fortresses, castles, etc.) is strongly affected by their dynamic interaction. At present, no codified and operational tools are available to perform the seismic assessment of such mutually interacting structures. This paper introduces a numerical procedure based on the use of nonlinear static analyses to fill this gap. The proposed procedure firstly requires the execution of a modal analysis on the 3D finite element model of the whole structure to define the modes which involve the dynamic response of each unit and their modal shapes. The latter are then fitted to define the load patterns to be applied on each unit through pushover analyses. The pushover curves obtained for each unit are then converted into capacity curves to finalize the seismic assessment. The effectiveness of the proposed procedure is shown through an application to a medieval fortress significantly damaged by the 2012 Emilia earthquake (Italy). The results achieved are promising and support the possible extension of the procedure to other typologies of complex historic structures composed by various interacting units.

Keywords: Interacting structures, Fortresses, Masonry, Seismic assessment, Nonlinear static analyses, Emilia earthquake.

1 Introduction

This paper deals with the seismic assessment of mutually interacting historic masonry structures carried out through nonlinear static analyses. This kind of structures is characterized by a seismic behavior which is ruled by the structural response of the many interacting units which form the whole building. This interaction can be relevant especially if the units are characterized by various architectural features that lead to different dynamic properties, stiffness and strength of the units. Such typology includes a huge number of examples: a bell tower incorporated in a church, monumental palaces which are often the result of subsequent additions of structural units, and fortified constructions (as fortress or castles), which are usually formed by towers connected through defensive walls (Fig. 1). Although the activation of local mechanisms is significant (e.g. mainly interesting out-standing portions such as battlements), the assessment of the global response is equally relevant. The paper focuses the attention only to the latter, particularly referring to the case of fortresses.

The vulnerability of fortresses was strongly highlighted by the 2012 Emilia earthquake [1]. In fact, such typology is particularly frequent in that area and offered several examples of severe damage, pointing out the complexity in interpreting their seismic behavior. A classification of the recurrent seismic damage mechanisms was originally proposed in [1], based on observed damage and typical configurations. In particular, the main observed mechanisms were: 1) damage mechanisms due to the interaction between the towers and the fortress' curtain walls; 2) damage mechanisms involving the main body of the towers; 3) damage mechanisms involving the upper parts of the towers; 4) damage mechanisms at the level of the roofs. Starting from the proposal of [1] for the Emilia fortresses, further damage mechanisms were then added in [2], corroborated by the damage collected for a large number of cases hit by other past Italian earthquakes across the whole country.



Fig. 1 - Examples of two Emilian fortresses: Vignola fortress (a) and Castello Estense in Ferrara (b).

The seismic assessment of such complex structures poses several critical issues. The first problem deals with the definition of the best modeling choice to be adopted that has to balance the need of a reasonable computational effort with that of guaranteeing a reliable assessment capable to catch the interaction effects. The second problem is instead connected to the lack of tools and standardized procedures to perform the seismic analysis and verification of such complex masonry structures [3]. While Standards [4] are more oriented to ordinary buildings, Recommendations addressed to monumental assets (i.e. [5]) in general state a

series of general principles and indications for possible methodologies of analysis, without however prescribing operational tools or indicating specific models and standardized procedures.

In this context, this paper aims to overcome the aforementioned lack of operational tools by proposing a procedure for the seismic assessment of mutually interacting masonry structures based on the use of nonlinear static analyses. The required steps of the procedure are explained in §2. The procedure is then applied to a case-study, which is the San Felice sul Panaro fortress (§3, §4, §5) that was significantly hit by the 2012 Emilia earthquake [1]. It is worth to note that the procedure uses a 3D finite element (FE) solid model of the entire structure, developed through a non-standard mesh generation procedure starting from a laser-scan survey, that allows to accurately describe the actual geometry (§4, [6, 7]). Therefore, in the whole model the dynamic interactions among the different units of the entire asset are explicitly accounted for. Furthermore, the use of efficient numerical algorithms keeps bearable the computational effort. The comparison between the occurred damage and the one predicted - in terms of crack pattern and ductility demand obtained by the analyses - allowed to validate the procedure (§6).

2 Seismic assessment of fortresses through nonlinear static analyses: Critical issues and new proposals

2.1 Modelling issues

The seismic assessment of complex monumental assets can be pursued by following two different approaches that affect also the choice in the modelling strategies: (i) the decomposition of the whole asset into different units (*e.g.* on the basis of historical and constructive features) by performing then separate verifications; (ii) the realization of a unique global model of the entire asset, performing the pushover analyses and, consequentially, making the verification through the capacity curve representative of the overall global seismic behavior. In principle, both alternatives can be considered reliable and have to be chosen depending on the specific features of the examined asset, on its complexity (that can make feasible only few alternatives) and on its expected structural behavior. However, they both present pros and cons. Regarding the first approach (i), the difficulties are mainly related to the need of defining the “equivalent” boundary conditions for each modeled unit. Obviously, as a consequence, such an approach is not able to consider the possible interaction effects between the different parts, unless in an approximate and conventional way. Conversely, the second one (ii) implicitly considers these interactions, although affected by computational effort complications induced by the modelling of the whole structure.

The seismic interaction of adjacent masonry structures is a very complex problem, given that the quality of the connection is difficult to evaluate and to mechanically describe; indeed, when it is really poor, a global behavior of the complete structure could not be activated. Despite that, the proposal of using a model of the whole structure is based on the idea of explicitly accounting for the effects of interaction that have been testified by various earthquakes, in particular in the case of fortresses which the paper focused on (as for many other Emilian fortresses [1] and many fortified constructions [2]). Furthermore, it has to be pointed out that:

- i) although the units are weakly connected, a certain interaction among them could appear when subjected to seismic action able to push one unit towards the other one and vice versa;
- ii) the dynamic behavior of this kind of structures, such as fortified structures, is highly dependent on the boundary conditions [1], thus an initial weak connection among units is not sufficient to guarantee a completely autonomous behavior of each sub-structure that is, neglecting mutual interactions;
- iii) relevant interactions can be determined especially if the units of the considered asset are characterized by different architectural features that lead to different dynamic properties, stiffness and strength of the units.

Of course, the numerical modelling of historic monumental structures, usually characterized by huge dimensions and complex and irregular geometries, represents a challenging task. The use of 3D solid finite elements with a continuum representation of the mechanical behavior of masonry, which allows to keeping affordable the computational effort [8, 9, 7, 10, 11, 12, 13, 14, 15], appears preferable than the adoption of more simplified modelling strategies, such as those based on the structural element approach, that are

particularly common in the context of ordinary buildings [16, 17]. Indeed, the latter appear questionable or to be carefully considered for the typology under examination since the common simplifications on which they are based, e.g. neglecting the out-of-plane response or the equivalent frame idealization, may result too rough and conventional in case of huge thickness of walls or presence of small openings, as the case of towers in fortresses.

The 3D solid geometry of these structures is usually developed in a CAD environment, which is generally an expensive and complex process with inevitable geometrical simplifications. However, recent mesh generation procedures allow to semi-automatically transform 3D point clouds, e.g. surveyed through terrestrial laser scanner (TLS), into solid numerical models, see for example [6, 7, 18, 19, 20].

In the following, between two approaches aforementioned, the second one (ii) is considered the most reliable for the fortresses which the paper focuses on and that are characterized by an aggregation of adjacent units (e.g. towers, curtain wall, buildings, etc.), which interact due to mutual boundary conditions. Indeed, the effects of adjacent buildings on the seismic behavior of a masonry tower have been discussed in [21], where the seismic behavior of a tower has been found to be considerably influenced by the presence of adjacent buildings. Particularly, in [21] it has been shown that the results obtained by numerical models which accounted for the adjacent parts were in good agreement with the damaged condition of an actual non-isolated tower that suffered an earthquake. However, the definition of equivalent boundary conditions to simulate the adjacent parts appears non-trivial and generally excessively approximated for this kind of structures. Therefore, the application of conventional boundary conditions on each unit of the structure appears inadequate and a comprehensive model of the whole structure is more appropriate to investigate its seismic behavior.

2.2 *Issues on analysis methods*

Once defined the most suitable numerical model, a further critical issue deals with the procedure for the analysis and verification, which is not manageable *a priori*. At present, Standards and Recommendations [4, 5] do not suggest a well-established procedure for the assessment of such complex structures. Linear analyses or methods based on the local verification of stress states can produce very conventional assessment since the redistribution effects are usually very significant. Furthermore, linear analyses need the adoption of a behavior factor which would be completely conventional for non-standard typologies as the one examined, being the values recommended in codes only calibrated for ordinary new buildings [22].

Thus, the use of nonlinear procedures appears essential to obtain more reliable results. In this framework, the options are two: nonlinear dynamic analyses (NLDA) and nonlinear static analyses (NLSA) based on the pushover framework.

NLDA are the most advanced analysis method today available. However, this procedure is not only computationally demanding, being not usually feasible even with very powerful computers in the case of very complex models, but it also presents some drawbacks.

On the one hand, only few numerical models allow to run time history analyses especially for masonry structures, due to the complexity of defining cyclic constitutive models and viscous damping models [23, 24]. Moreover, the energy dissipation due to impacts between structural units, the pounding between adjacent structures and the damping model for masonry structures are still challenging aspects to account for.

On the other hand, the choice of suitable accelerograms sensibly influences the response of the structure and, so, the results of the analyses, due to the well-known record-to-record variability. This issue is particularly tricky when a limited number of records is adopted, as usually suggested in Standards (e.g. 7 different accelerograms for the Italian Standards) and implied by the huge computational effort required by the so complex models discussed in this paper.

Additionally, safety assessment procedures are still under investigation for dynamic analyses of masonry buildings and, for monumental structures, this is even more challenging representing still an open issue, both in literature and in Standards [23, 25]. In fact, currently no Standards propose operative tools to perform the seismic verification of monumental structures through NLDA. Furthermore, if the final goal is to perform a seismic assessment (and not strictly a verification given a precise seismic demand), the results of NLDA have to be finalized to evaluate the maximum acceleration compatible with the fulfillment of a target limit state (LS). In general, evaluating the maximum acceleration compatible with the fulfillment of a target LS by using NLDA requires to perform incremental dynamic analyses (IDA) or multiple stripes analyses, both characterized even by a more significant computational effort. Finally, but not secondary, the interpretation of the huge amount of information of the NLDA results is not straightforward to be defined with the aim of carrying out a performance-based assessment especially for monumental buildings: that is at the same time the most crucial aspect, since it represents the main tool to plan strengthening interventions [23, 25].

For these reasons, the use of NLSA is considered an effective tool [26] and it represents the most widespread method to study the global response of existing buildings, as well. A critical review of its reliability in case of ordinary regular and irregular masonry buildings has been illustrated in [27, 28].

The main assumption of pushover-based methods is that the structure vibrates predominantly in a single mode. For this reason, NLSA is usually based on the application of a unique force distribution (for example proportional only to mass or proportional to mass and elevation). Then, most Standards propose to apply at least two different load patterns (LP) or a combination of force distributions to approximately consider the evolution of inertial forces which depends on the progressive degradation of the structure. However, the use of a single LP on the whole model risks to be too conventional in a pushover analysis framework. Indeed, it could fail in activating the nonlinear behavior of all the units in the aggregate. For example, when the most vulnerable units of the structure exhibit a nonlinear behavior, the others can almost remain in the elastic field. Furthermore, this assumption may not be fulfilled, especially in high-rise buildings, where higher modes effects may be important along their height [29]. However, both in low-rise buildings (like the majority of ordinary masonry structures) and in more complex structures (like the monumental ones) higher modes effect

may be significant, due to the presence of in-plan irregularities (which induce torsional effects) or of flexible diaphragms (then, the first mode does not activate all the walls) [28].

Other strategies in the field of NLSA as the multimodal or adaptive approaches have been mostly developed for other structural types (reinforced concrete and steel buildings) and their application to masonry is still under investigation even for simple structures [30] having produced results not so encouraging in previous applications [31].

The second problem is connected to the availability of robust criteria to define proper performance levels on the pushover curve in case of complex masonry buildings. In the case of other typologies, e.g. RC buildings, the structural elements are usually modeled without a post-peak strength degradation and the seismic verification is developed through local safety checks. This procedure is not suitable for unreinforced masonry buildings, since their structural elements often present a significant strength degradation that needs an analysis involving the building in its entirety. Criteria to define performance levels that combine checks at different scales (that of structural elements, the one of whole walls and the global one) have been recently proposed in [26].

Finally, in order to evaluate the seismic demand corresponding to the attainment of the different performance levels, the NLSA needs a procedure to compare the capacity with a response spectrum. To this aim, firstly, the pushover curve representative of the behavior of the multi-degree of freedom system (MDOF) has to be transformed into the capacity curve of the equivalent single-degree of freedom one (SDOF) and, then, a procedure to properly reduce the elastic spectrum has to be adopted. Concerning the latter issue, several methods are proposed in literature and Standards (as the Coefficient Method in [32], the N2 Method in [33], the Capacity Spectrum Method in [34]). Recent works highlighted how, among them, in case of structures characterized by a short period as the masonry structures the N2 Method risks to produce assessment not conservative [27, 28, 35]. Therefore, at §6.1 of this paper the adoption of the Capacity Spectrum Method will be favored.

2.3 Adopted procedure

In order to face the aforementioned issues and to provide a first contribution to overcome the lack of operational tools identified in literature, this paper proposes a procedure for the seismic assessment of irregular complex structures together with a first application to the case of fortresses. The procedure follows five steps:

1. Generation of a FE model of the whole aggregation of units aimed at explicitly capturing the mutual interaction effects;
2. Execution of a modal analysis to define the modes involving the dynamic response of all the units and their modal shapes;
3. Fitting of the modal shapes to define the LP distribution to be applied to each unit that may vary in plan and height;

4. Execution of a series of pushover analyses (for each unit) by applying to the whole numerical model the force distribution obtained from the modal shapes identified in 3), which generally involves only one unit;
5. Conversion of the pushover curve of each unit in the capacity curve representative of the equivalent SDOF system and then finalization of the seismic verification.

Fig. 2 sketches the proposed procedure, applied to San Felice sul Panaro Fortress, which is the case study considered in the Sections below. The proposed procedure is general and potentially applicable through several numerical modelling strategies [36, 26], e.g. discrete element method (DEM) based approaches [37].

It has to be pointed out that devising the various units and the loading to be applied in each pushover analysis presupposes the analyst's interpretation of the global modal configurations. However, the few practical guidelines listed below can help in the definition of the different units:

- for the standardized building typology object of the paper (the fortified buildings, including castles, fortresses, and citadels), the post-earthquake damage systematically highlighted their propensity to exhibit an independent dynamic behavior of the towers, which are affected by the dynamic interactions with the adjacent structural bodies [2, 1]. This dynamic behavior is mainly due to: i) the architectural transformations occurred over the centuries which led to the actual structural configuration, mostly formed by towers connected through massive defensive walls; ii) the different dynamic properties, stiffness and strength which characterize the different units, thus determining these significant dynamic interactions. In this case, the experience from the damage observed after past earthquake can primarily address the analyst (and addressed the Authors in this specific case) in the identification of the units;
- more in general, when there is no evidence of the dynamic behavior by the post-earthquake damage or for other building typologies (such as aggregates, monumental palaces or bell towers incorporated in a church) which are not characterized by recurring and standardized architectural configurations, identifying the various units can be not so trivial. However, also in these cases, a deepen preliminary analysis on the historical transformations faced over the-centuries and the analysis of their peculiar constructive features (also through in-situ investigations) can help the analyst to identify the various units and outline the most reliable hypotheses on their mutual interaction.

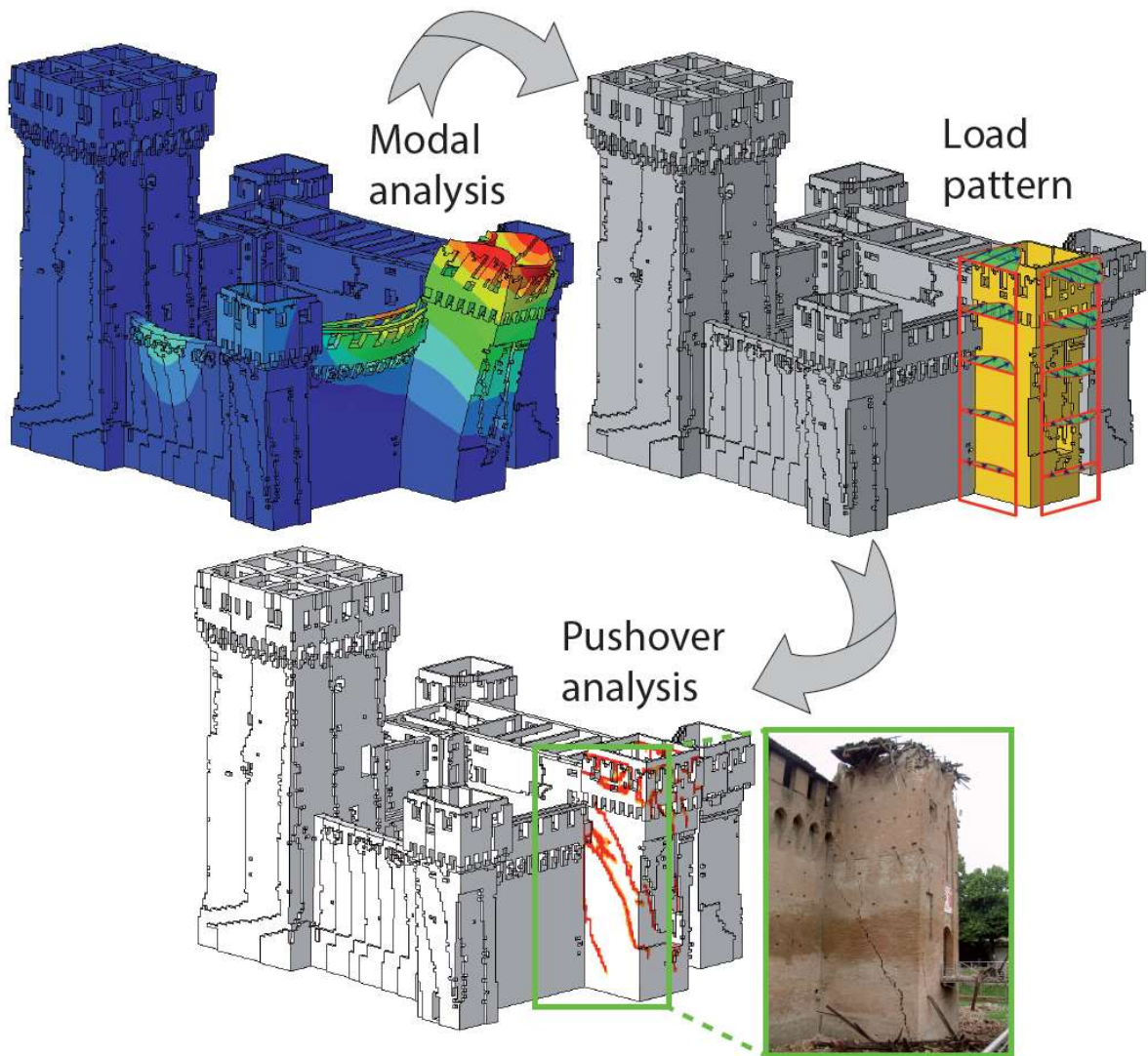


Fig. 2 - Sketch of the proposed procedure.

3 The case-study of San Felice sul Panaro fortress

The San Felice sul Panaro fortress is located near the city of Modena in San Felice sul Panaro (Italy), which has been severely hit by the 2012 Emilian earthquake. It represents a typical example of Emilian fortified medieval architecture, composed by a very massive main structure, characterized by a compact quadrilateral plan with an inner yard and five towers: four of them are localized at the corners, while the other one is placed on the north fortress façade (Fig. 3). The S-E tower is called “Mastio” (the keep), since it has a dominant dimension if compared to the rest of the structure. The masonry is made by solid bricks and lime mortar, as usual in all the constructions of the area. Masonry cross section is usually solid, even if the central part is often made of reused bricks and poor lime mortar.

The San Felice sul Panaro fortress shows a complex historical evolution during the centuries. The current configuration of the fortress dates to the 14th-15th century [38]. At the beginning, the fortress probably had a quite simple shape, with a quadrilateral walled enclosure and a tall sighting bastion. In the following century, the fortress, which assumed the present configuration, was restored and fortified [38]. Later on, other buildings were built in the inner courtyard. More recently, starting from the 1960s, some modern interventions were realized, such as a concrete curb on minor towers and Mastio trunk reinforcement.



Fig. 3 - North façade of San Felice sul Panaro Fortress (view before the Emilia earthquake, 2012) and schematic floor plan.

3.1 Damage pattern after the Emilia earthquake

In May 2012, the Emilia earthquake hit the San Felice sul Panaro fortress. The epicenters of the first (May 20th) and second (May 29th) main shocks were about ten and five kilometers far from the fortress, respectively. The seismic sequence induced the collapse of the four minor roofs of towers (Fig. 4a), shear cracks of different relevance on the main body of the Mastio (Fig. 4b) and of the other towers and extensive collapse in the north tower, this latter induced by the shock of May 29th (Fig. 4c). It has to be pointed out that the different seismic behavior exhibited by the five towers was highlighted by: the different interventions they were subjected to; the different position in plan and the different connection quota with the perimeter wall (which determined irregularities in plan and in elevation); the quality of connection with the other fortress structures.



Fig. 4 - Collapse of a minor tower's roof (a), damage pattern in the Mastio (b) and collapse in the north tower (c).

Furthermore, serious damage occurred in the lower part of the S-E tower, characterized by the presence of wooden floors or vaults. For example, some deep cracks occurred in the vault of the Giulio II Hall (Fig. 5a) and the perimeter walls detached from the floor of some centimeters (Fig. 5b). Then, a significant damage was concentrated also in the battlements (mainly shear diagonal cracks in the Mastio merlons and horizontal cracks in the North perimeter wall – see Fig. 5c-d, respectively) and in the masonry corbels that support the upper parts. Finally, the earthquake induced the detachment between perimeter walls and towers and the out-of-plane response of the West wall in two levels. A more detailed description of the exhibited damage mechanisms is contained in [1]. Despite the general overview of damage provided, in the paper the attention is focused to the in-plane global response of structural units rather than on the local mechanisms activated in battlements or local portions according with the main aims of research herein described.

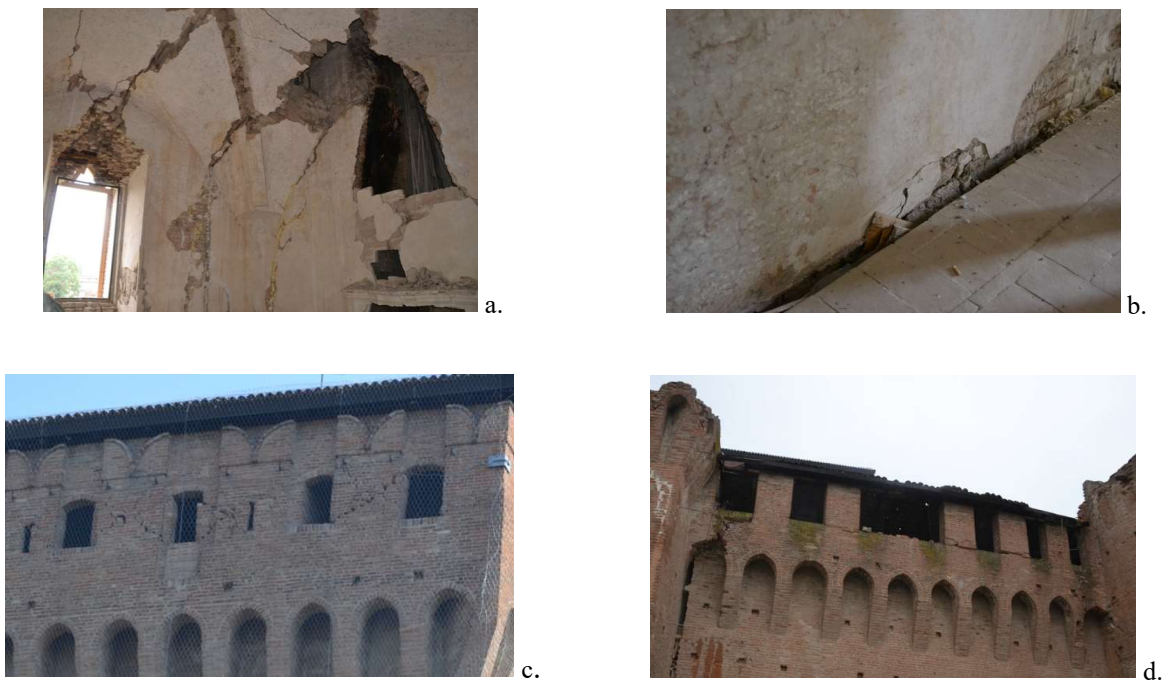


Fig. 5 - Damage pattern in the Giulio II Hall (a-b) and in the battlements (c-d).

4 The numerical model of the fortress

The finite element model of the fortress in San Felice sul Panaro has been developed by means of a non-standard mesh generation procedure called CLOUD2FEM, conceived and set up by part of the Authors in [6, 7]. Such an original procedure semi-automatically transforms 3D point clouds of complex geometries in 3D FE models, keeping low the user-time demand with respect to traditional CAD-based approaches. In this section, the FE mesh generation of the case study is briefly revisited. The interested reader is referred to [6, 7] for further details. Furthermore, the description of the adopted constitutive law for masonry, as well as the verification of the consistency of its mechanical parameters, are reported. Finally, the load pattern implementation and the analysis algorithm adopted are discussed.

4.1 FE mesh generation

In the aftermath of the 2012 Emilia earthquake, the municipality of San Felice sul Panaro commissioned a laser scanner survey of the fortress' outer and inner surfaces to acquire a detailed snapshot of its condition (Fig. 6). Firstly, the surveyed points cloud (Fig. 6a) has been processed by standard operations, *i.e.* the reduction of the points' density and the generation of the triangular irregular network (TIN) mesh. Then, the TIN mesh (Fig. 6b) has been broken down in 2D subdomains by slicing it perpendicularly to the vertical direction with a 25cm step. The boundary polygons, which enclose the outer and inner points of each slice, have been computed by means of a concave hull algorithm, generating filled regions [6, 39]. Afterwards, each slice has been transformed into a digital image composed of pixel with a 25x25cm resolution. As the digitalization has been performed of a fixed region of space, the slices were stackable and the subsequent stacking operation generated voxels. Finally, each voxel has been converted into an eight-node hexahedral finite element and, hence, the structure has been completely discretized as a unique continuum composed by evenly spaced hexahedral elements. The adopted 25x25x25cm resolution was found to be by the authors the best compromise between accuracy and computational effort for the case under study [7, 18].

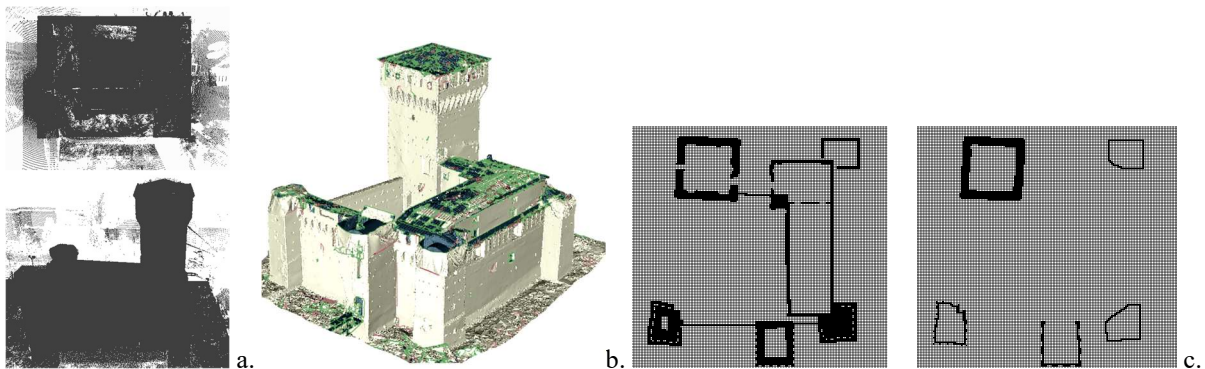


Fig. 6 - Laser scanner survey of the fortress: (a) points cloud, (b) TIN mesh and (c) example of processed slices.

Although the laser scanner survey was conducted for both the interior and exterior surfaces of the building, several criticalities had to be addressed. Indeed, there were debris and piles of rubble in the surroundings of the building, and there was furniture in several rooms of the building. These disturbing elements hid the actual geometry of the building. Therefore, a manual processing of the slices was required to keep the non-structural

portions out of the geometry. Even if this part of the procedure is semi-automatic, some manual interventions appeared fundamental for a precise separation between non-structural and structural parts. Despite the survey and, hence, the generated model were based on the after-quake condition of the structure, it was possible to include the collapsed portions of the fortress in the FE model to obtain its before-quake condition. Indeed, by processing the 2D slices in a voxel framework, the lacking parts of the structure have been geometrically modeled with reference to a before-quake documentation (drawings, plans and photos). Fig. 6c shows two examples of processed slices in which the geometry of the minor towers' crowning (collapsed due to the seismic events) has been recreated with a reasonably good approximation. Such an operation was facilitated by the peculiar mesh regularity, which helped the user in the geometrical reconstruction.

Fig. 7 shows the obtained 3D FE model of the fortress. The whole model counts 526,985 nodes and 424,096 eight-node hexahedral elements.

It has to be pointed out that the raw semi-automatic procedure leads to a simplification of the geometry by approximating the external surface with a regular grid-based mesh. This simplification then introduces some discontinuities on the FE model that are more visible where the structure is irregular with respect to the main direction used to generate the grid. In general, for skew geometry, the first raw approximation can be easily enhanced by means of standard mesh improvements [6].

As can be noted from the magnified portion in Fig.7, the adopted discretization is quite fine aiming at investigating the fortress global structural behavior. Indeed, all the structural elements of the fortress present at least 2-3 hexahedral elements along the walls' thickness. Exception is made for the minor towers crowing's walls, where in some portions only one element along the thickness is present. However, following the aforementioned scope, this condition can be tolerated.

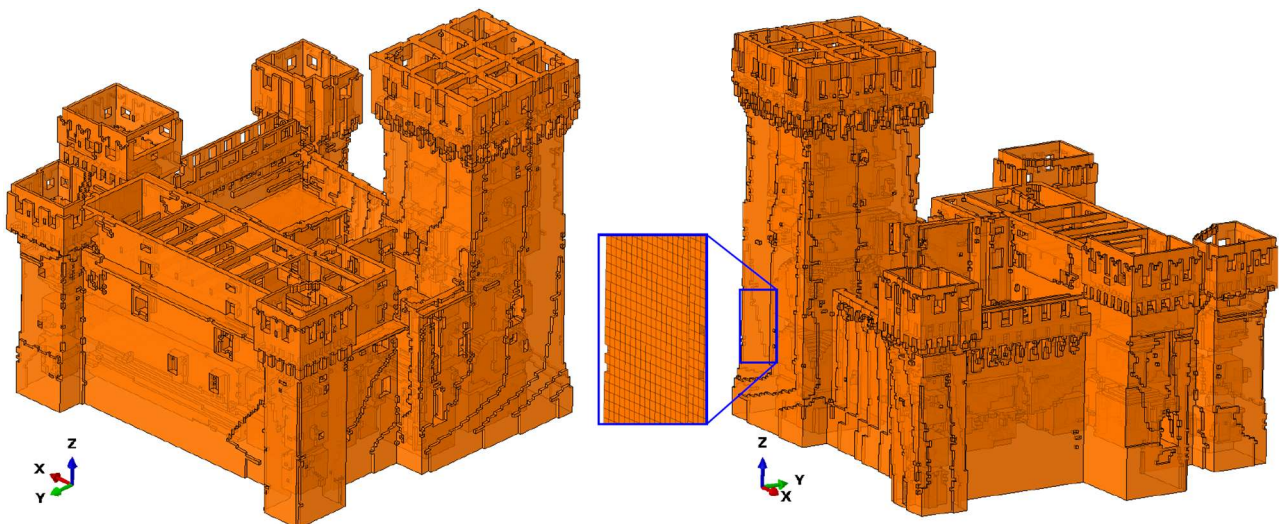


Fig. 7 - 3D finite element model of the fortress. The magnified portion shows the adopted discretization.

According to the adopted mesh generation approach, floors and vaults are automatically meshed through solid 3D FE in a jagged representation of the original geometry. In this case, instead of using equivalent diaphragms to model floor and vaults [16], 3D solid jagged elements are used to approximately account for the presence

of floors and vaults. Such approximations, however, can be considered satisfactory aiming at investigating the global structural response.

The effectiveness of the model generated is also shown in [40], where the model, in the after-quake condition, has been updated with ambient vibration data measured on the Mastio. Indeed, the capability of adequately reproduce the first five natural frequencies and modal shapes of the Mastio showed the reliability of the FE model, as further described at §4.2.

The fortress under study is a very complex building composed by several materials. For simplicity, four different material properties have been identified and implemented in the FE model (i.e. masonry, timber, reinforced concrete and terrain). Particularly, the last three materials have been assumed linear elastic, for simplicity. Conversely, the nonlinear behavior of masonry is described at §4.2. It has to be noticed that, in order to do not alter the linear dynamic response of the structure (e.g. in terms of participating masses), the terrain, which is present in the courtyard of the building (with a level at approximately 3.50 m higher than the external one), has been considered with a very small density.

The model is assumed on a fix base. Indeed, although for massive structures as the fortresses the soil-structure interaction could be significant [41, 42], this assumption is considered reliable for the San Felice sul Panaro case study, since the soil at the fortress foundation is not poor quality and no damage caused by soil-structure interaction problems has been highlighted on the structure.

4.2 *Constitutive model for masonry and mechanical parameters adopted*

The nonlinear behavior of masonry emerges also for stress states substantially lower than its maximum strength. As known, masonry is characterized by different strengths in compression and in tension, with the latter considerably lower than the first, and by anisotropic behavior, both in linear and nonlinear regimes, due to the heterogeneity of the material composed by bricks and mortar joints [43].

Detailed models that account for the actual texture of masonry have a long tradition in the scientific literature [44]. Additionally, orthotropic continuum damage models have been successfully formulated for masonry [45]. However, these sophisticated approaches appear too computational demanding to analyze actual large-scale structures. Additionally, the assumption of orthotropic nonlinear behavior generally appears as questionable as an isotropic one for historic masonries, since they are usually characterized by chaotic and random textures [9, 8, 46, 19].

In this paper, the isotropic plastic-damage constitutive model developed by Lee and Fenves [47] for quasi-brittle materials is adopted for masonry. In the following, the main features and parameters involved in the model are recalled. The interested reader is referred to [47, 9] for further details.

Two independent scalar damage variables are supposed. Particularly, one scalar damage variable for the compressive behavior ($0 \leq d_c < 1$) and one for the tensile behavior ($0 \leq d_t < 1$) are employed. According

to the concepts of effective stress and strain decomposition, the stress-strain relations under uniaxial compression, σ_c , and tension, σ_t , are:

$$\sigma_c = (1 - d_c)E_0(\varepsilon_c - \varepsilon_c^p), \quad \sigma_t = (1 - d_t)E_0(\varepsilon_t - \varepsilon_t^p), \quad (1)$$

where E_0 is the initial Young's modulus of the material, ε_c and ε_t are the uniaxial compressive and tensile strains, and ε_c^p and ε_t^p are the uniaxial compressive and tensile plastic strains (Fig. 8). In particular, the curves shown in Fig. 8 denote the main input data required by the model.

The constitutive model is formulated in the context of non-associated plasticity [47]. Therefore, the plastic potential is characterized by the dilatancy angle ψ , generally assumed equal to 10° for masonry [48], and by a smoothing parameter ϵ usually assumed equal to 0.1 [9]. A multiple-hardening Drucker-Prager type surface is assumed as yield surface. This surface is specified by the ratio f_{b0}/f_{c0} between the biaxial f_{b0} and uniaxial f_{c0} initial compressive strengths and a constant ρ , which represents the ratio of the second stress invariant on the tensile meridian to that on the compressive meridian at initial yield. The values $f_{b0}/f_{c0} = 1.16$ and $\rho = 2/3$ are typically adopted for masonry [9].

As regards the mechanical parameters, the in-situ investigations carried out on the Fortress (double flat-jack, shove test, compressive tests on drilled specimens, etc) shown a broad set of results for which the definition of a precise set of values of mechanical parameters was not possible (e.g. the compressive strength of masonry). Despite that, such results were useful to support qualitative evidences and address the choice of parameters within some reference values proposed in the literature for similar masonry typologies.

In particular, the Italian code [49, 50] provides mechanical properties for several representative masonry typologies which can be found on the Italian territory, including the clay brick and lime mortar masonry type that characterizes the San Felice sul Panaro fortress.

According to range of variation proposed in the Italian Code, the value 1500MPa has been adopted as Young's modulus of masonry. This value is referred to the undamaged state of masonry. Contextually, the overall Young's modulus of the Mastio in the after-quake condition has been estimated in [40] through an ambient vibration-based FE model updating. The resulting value, representative of the damaged state of masonry, has been found to be equal to the 55% of the one adopted in this paper. Although a direct and conclusive correlation between these two works is not possible, this result somehow supports the reliability of the value adopted for the Young's modulus, which is consistent with the masonry typology under examination and for which such a reduction could be reasonable, given the highly-damaged state of the tower (Fig. 4b).

The adopted compressive and tensile uniaxial stress-strain relationships are shown in Fig. 9, leading to an indirect definition of the fracture energies in tension and compression. Particularly, the values 2.40MPa and 0.12MPa have been assumed as uniaxial compressive and tensile strengths, respectively [49, 50]. In particular, the adopted value for the compressive strength (2.40 MPa) is the minimum value suggested by the Italian code [49, 50] for the clay brick and lime mortar masonry type. This choice is justified by the fact that the absence of plaster in the examined masonry and the oldness of this building, together with very limited maintenance

over the centuries (as testified in other Emilian fortresses, as well), might have facilitated the decay of the mortar and consequently the reduction of mechanical characteristics of the masonry.

The evolution of the scalar damage variables d_t and d_c , as function of the uniaxial strains, has been kept substantially proportional to the decay of the uniaxial stresses (Fig. 9), as adopted in several numerical campaigns of masonry structures [21, 46, 51, 41]. Although stress states in fortified masonry structures are usually far from compressive failures in static conditions, when these structures are pushed horizontally their compressive stresses significantly increase. Therefore, compressive softening is herein accounted for.

A summary of the adopted mechanical parameters is collected in Table 1. The effectiveness of the constitutive model employed for masonry and of the mechanical parameters assumed with respect to the consequent strength predictions at the scale of masonry panels is shown in the following section (§4.3).

Finally, it has to be pointed out that the walls of the San Felice sul Panaro fortress are characterized by multi-leaf brick masonry. Despite in some portions of the building an out-of-plane damage of the external leaf has occurred [52], the main scope of the paper consists in analyzing the global response of the units and to outline a procedure to account for their interaction in their safety assessment.

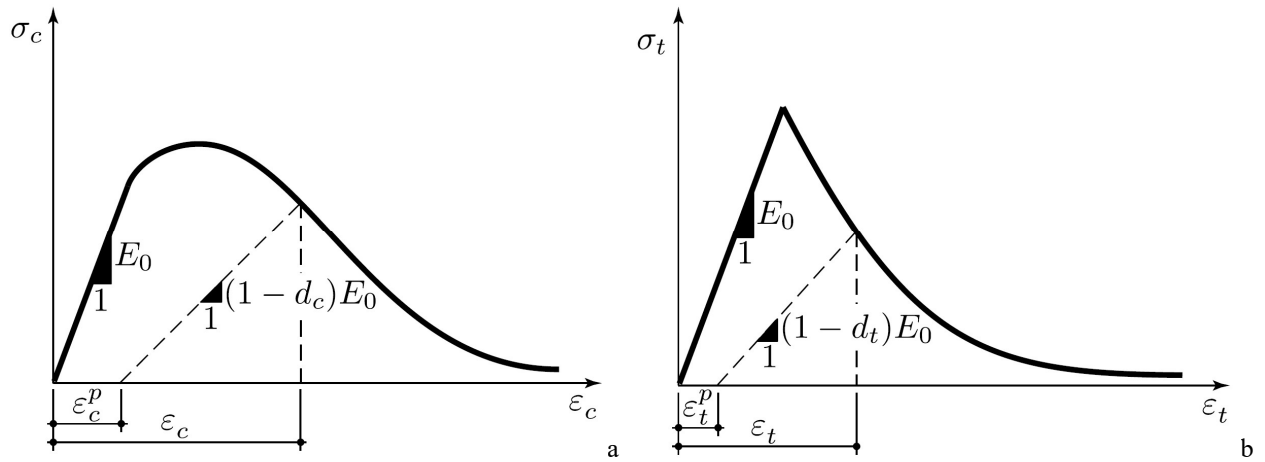


Fig. 8 - Plastic-damage constitutive law for masonry: a) compressive and b) tensile uniaxial stress-strain relationships.

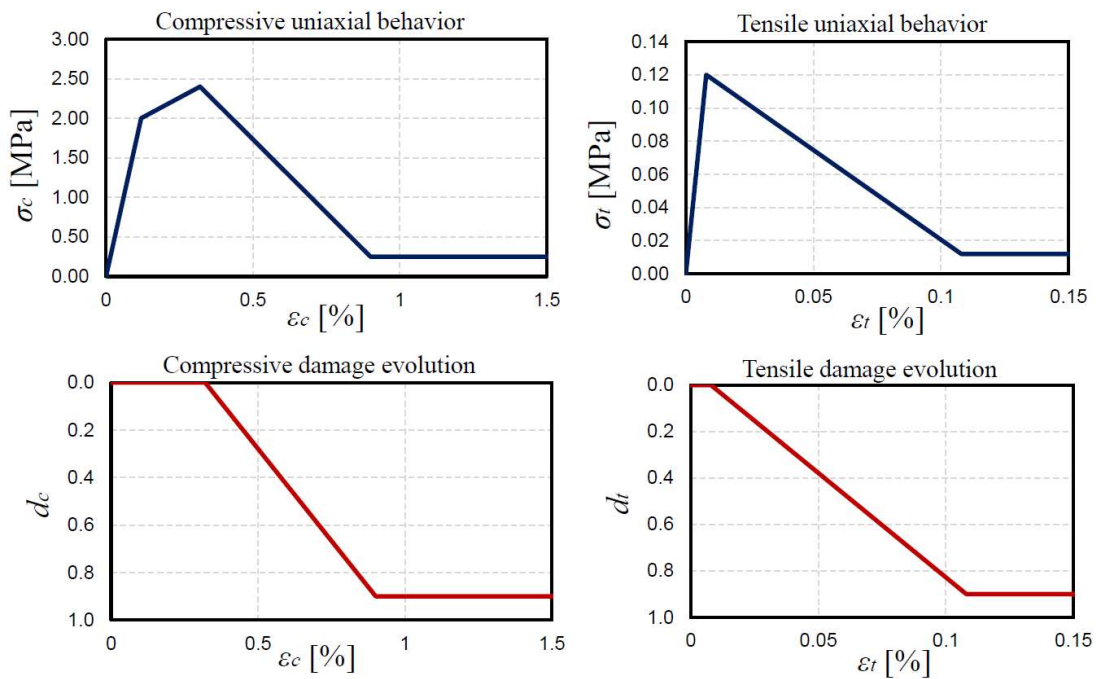


Fig. 9 - Uniaxial behavior and damage evolution for the compressive and tensile regimes.

Table 1. Masonry mechanical parameters.

Young's modulus [MPa]	Poisson's ratio	Density [kg/m ³]	ϵ [°]	ψ [°]	f_{b0}/f_{c0} [°]	ρ [°]	VP [°]
1500	0.2	1800	0.1	10°	1.16	2/3	0.002

4.3 Mechanical parameters consistency

The definition of reliable mechanical properties for existing masonry structures is a challenging task. This is even more complex when dealing with historic structures, where *in situ* destructive tests are limited or often forbidden. Therefore, reference to literature or codes material properties is usually undertaken, as also herein adopted and afore illustrated in §4.2. However, such parameters, and in particular those associated to the interpretation of the shear failure modes (e.g. shear strength), are usually referred to the scale of masonry panels rather than the scale of the material, as contemplated instead in continuum FE formulations. Thereby, the evaluation of the consistency of the adopted mechanical parameters with consolidated panel-scale strength criteria appears of primary importance. To this aim, a simple benchmark of a masonry panel (Fig. 10) has been modelled. The numerical outcomes obtained on the benchmark have been compared with well-known shear-strength criteria, as the ones contemplated in the Italian code [49, 5]. Fig. 10a shows the mesh used and its geometrical dimensions. Blue elements represent rigid links. The implemented mesh corresponds to the discretization adopted in the fortress model (i.e. 25x25x25cm). The masonry panel has been subjected to vertical compressive normal stress coupled with shear stress. Several simulations have been carried out with different values of the vertical normal stress in order to simulate the whole strength domain of the panel. Typical tensile and compressive damage contour plots at failure are shown in Fig. 10b and Fig. 10c, respectively.

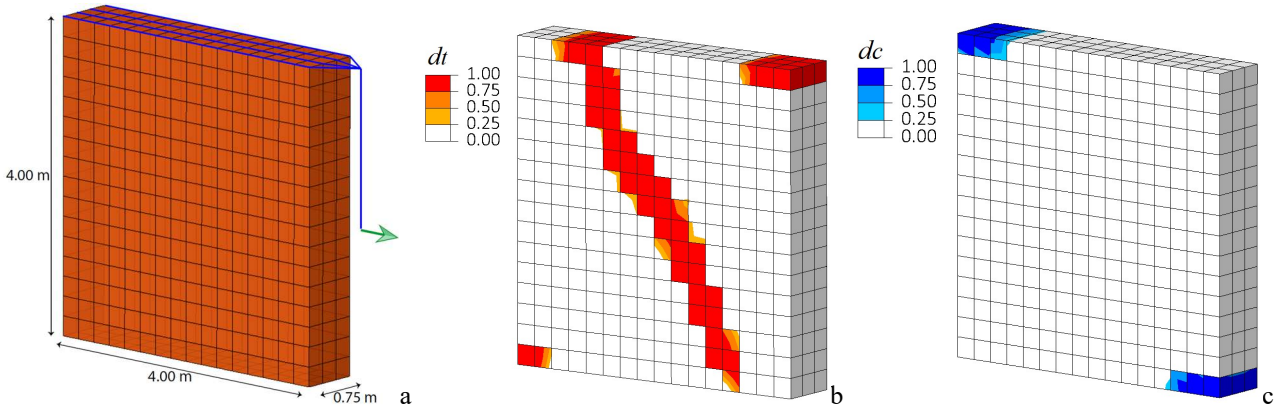


Fig. 10 - Benchmark used for the verification of the mechanical parameters: (a) 3D mesh, examples of (b) tensile and (c) compressive damage contour plots at failure ($\sigma/f_m = 0.43$).

Numerical findings, in terms of ultimate shear, have been compared with two well-known shear strength domains, which are contemplated in the Italian code [49, 50, 5], see Fig. 11. In particular, the Turnsek-Cacovic [53] criterion with the modification then introduced in [54], (2), and the criterion based on the failure due to combined compressive and bending stress, (3), have been considered:

$$V_u = \frac{1.5\tau_0 B t}{b} \sqrt{1 + \frac{\sigma}{1.5\tau_0}} \quad (2)$$

$$V_u = \frac{\sigma B^2 t}{2} \left(1 - \frac{\sigma}{0.85f_m}\right) \frac{1}{B/2} \quad (3)$$

where V_u is the ultimate shear, τ_0 is the masonry shear strength without vertical normal stresses, B is the length of the panel, t is the thickness of the panel, σ is the average normal vertical stress and b is a corrective coefficient assumed equal 1. For τ_0 the value 0.08MPa has been assumed according to [50] for clay brick masonry with weak mortar and quite regular texture. As can be noted in Fig. 11, a good agreement between the FE results and the Turnsek-Cacovic shear-strength criterion can be observed. It has to be pointed out that the criterion defined in (3) is based on the conservative hypotheses of no-tension material and stress-block behavior in compression. Therefore, the slight overestimation of the numerical results with respect to (3) for very low or very high compressive stress appears reasonable and expected.

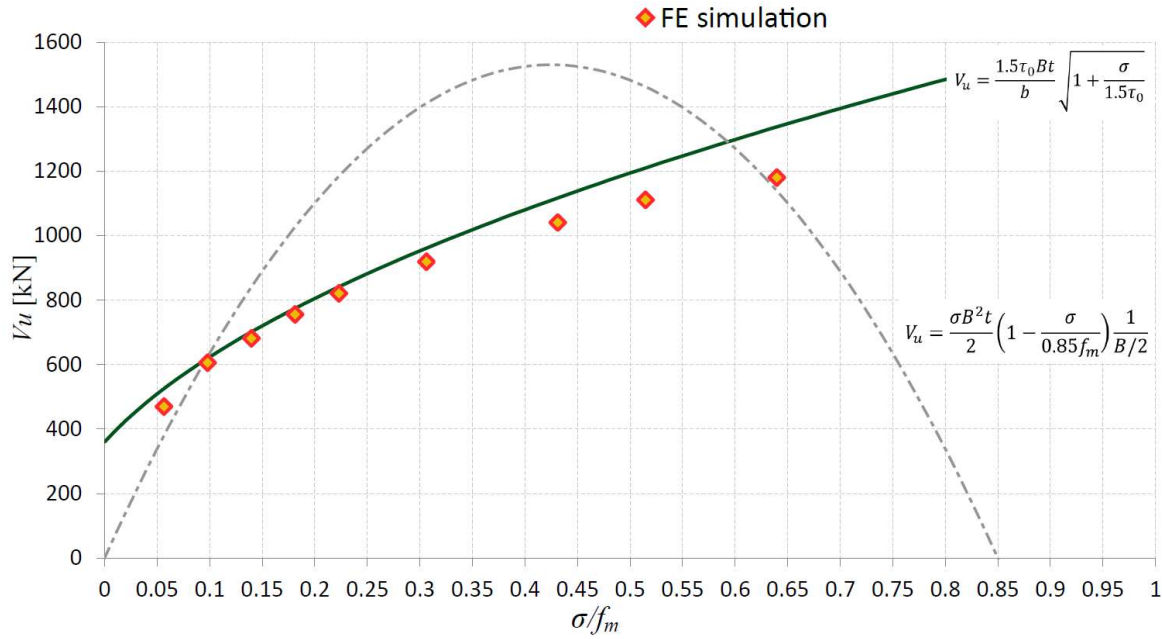


Fig. 11 - Ultimate shear comparison between strength domains for masonry panels and the results of FE simulations.

Moreover, in order to evaluate the effectiveness of the adopted mesh size and the role of the regularization introduced by the viscosity parameter (VP), a set of analyses have been conducted with progressively finer mesh generated by subdividing each 8-node hexahedral element into four FEs the with orthogonal vertical planes for the sake of comparison. The analyses have been performed on the FE model of the SW tower, which was extracted from the whole model. The same LP for the SW tower was considered in all the analyses. In particular, this LP is characterized by two trapezoidal distributions in plan (towards N and W) which exponentially vary in height. The results of the analysis, in terms of pushover curves and tensile damage contour plots, are shown in Fig. 12, whereas the times required by the numerical analyses are collected in Table 2 together with the sensitivity analysis on the viscosity parameter VP. By inspecting Fig. 12 it is possible to see that there is no particular influence of the mesh size on the pushover curve and on the cracking pattern, confirming the capability of the mesh adopted to represent complex stress gradients.

In particular, a very good agreement is observed in the damage patterns of the finer and reference meshes, which point out the same cracks in mostly the same positions. Also, the differences of the pushover curves, in terms of maximum base shear are substantially small, included, in the Authors opinion, in between the

constitutive law approximations. Finally, by inspecting Table 2, a considerably better efficiency of the reference mesh is observed. Indeed, the time needed by the reference mesh is much lower than the one needed by the finer mesh. Therefore, the chosen mesh appears a good compromise between results accuracy and computational effort for the case under study.

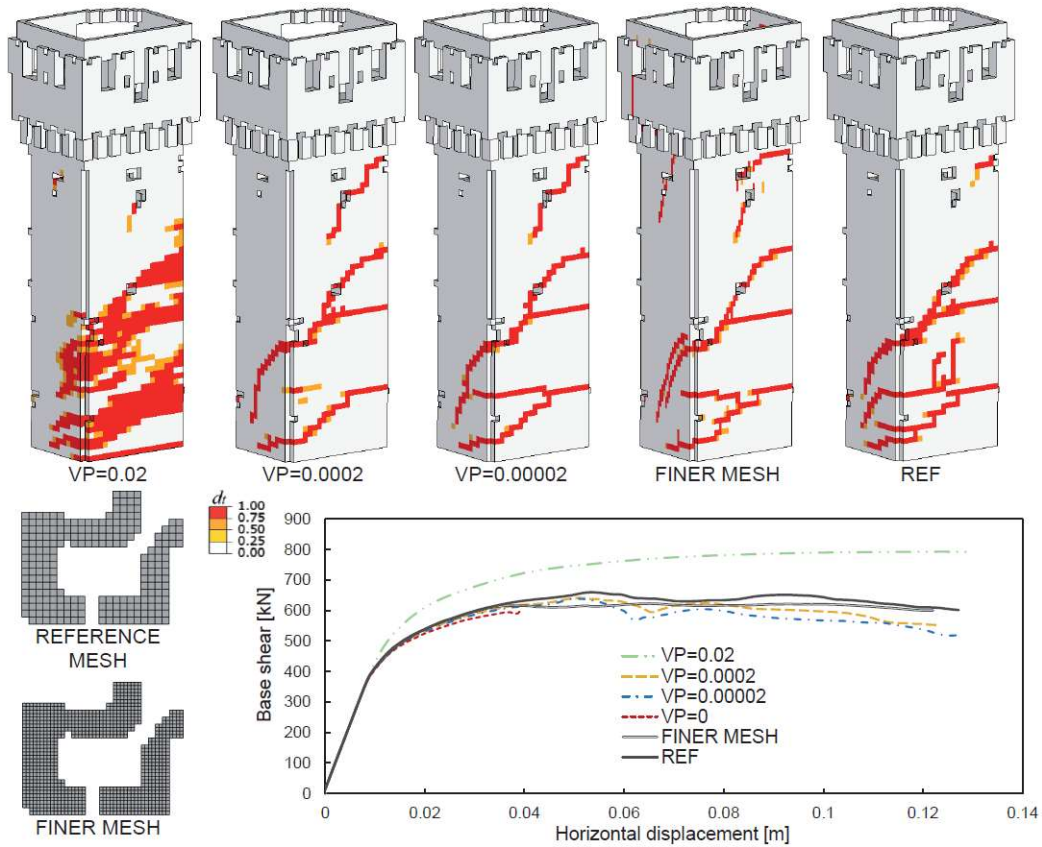


Fig. 12 - Sensitivity analysis on viscosity parameter and mesh size. The tensile damage contour plots are referred to a top horizontal displacement equal to 0.08 m.

Table 2. Times required by the numerical analyses.

Analysis	VP	Time required ^(x)
REF	0.002	00:41:05
FINER MESH	0.002	11:28:44
VP=0	0	Diverged
VP=0.00002	0.00002	04:38:13
VP=0.0002	0.0002	03:09:56
VP=0.02	0.02	00:27:12

^(x) on a commercial laptop equipped with a processor Intel®Core™ i7-6500U CPU @ 2.50GHz and 16GB RAM.

4.4 *Load application and analysis procedure*

The FE model depicted in Fig. 7 has been imported into the software Abaqus Standard [55], which has been used to perform the pushover analyses. The Italian Tier-1 cluster (GALILEO), devoted to scientific computing on the basis of national and European proposals (recently introduced in CINECA), has been exploited to conduct the simulations. Particularly, an 8-nodes supercomputer (RAM 128 GB per node) with two 8-cores Intel Haswell (2.40 GHz per node) has been utilized. Each pushover analysis lasted for 24 hours.

A two-step analysis approach has been implemented. Firstly, gravitational loads are applied to the structure. Secondly, non-uniform-distributed element-based horizontal loads have been applied through user-defined subroutines, following the LPs defined from the modal analysis.

To compute the solution up to the collapse of the structure (also in case of softening), a quasi-static direct-integration dynamic analysis algorithm has been adopted [55]. This algorithm allows to analyze quasi-static responses in which inertia effects are essentially introduced to regularize unstable behaviors. The Authors experienced a better performance of this algorithm, specifically in the softening regime, with respect to more common arc length procedures. Geometric nonlinearity has been considered in the analyses to account for large-displacement effects.

5 Application of the proposed procedure to the case of the San Felice sul Panaro fortress

The San Felice sul Panaro fortress is composed of an aggregation of units (towers, curtain walls and recently added buildings) which exhibited an own behavior although strongly influenced by their mutual interaction. In addition to the preliminary analysis of the historical transformations faced over the-centuries by the fortress and of their structural details, the identification of these various substructures has been benefitted, in the examined case, also from the interpretation of the surveyed damage pattern (§3).

In the following sections, the steps of the procedure introduced in §2 are hereinafter illustrated referring to the units identified in Fig. 13.

1. North (N) tower
2. North-West (N-W) tower
3. South-West (S-W) tower
4. Mastio
5. North-Est (N-E) tower
6. West unit
7. North wall
8. Construction named “Casa Matta”
9. East wall
10. Entry unit

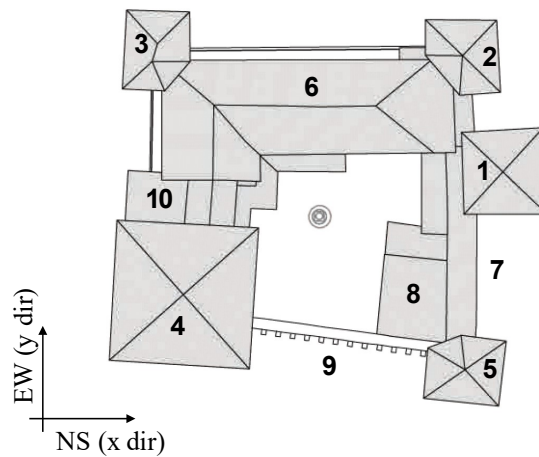


Fig. 13 - Identification of the main units in the San Felice sul Panaro fortress.

5.1 Definition of the load patterns

Once identified the main units of the structure (see Fig. 13) and realized the 3D model of the whole structure (§4), the procedure requires to perform a modal analysis to define the modes involving the dynamic response of all the units and their modal shapes (Table 3). Rather than considering the modes with a significant participant mass with respect to the global structure, the modes which activate a significant mass with respect to each examined unit are considered to define the load patterns; to this aim, the participant factor e^* is evaluated with reference to the mass of the unit under investigation. Table 4 presents in particular: the units under investigation (use Fig. 13 for the ID number); the selected mode/modes for each unit, together with the main direction/directions in which the mode is activated; the analysis directions; the mass participant factor e^* ; the period T and the

Table 3. Modal shapes of the selected modes for each examined unit.

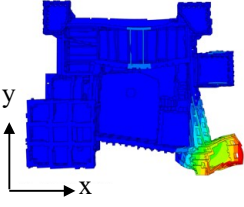
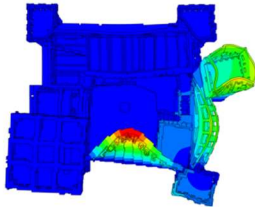
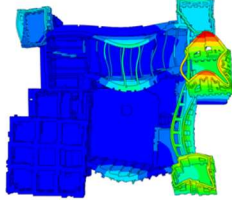
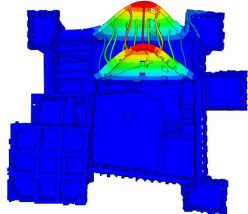
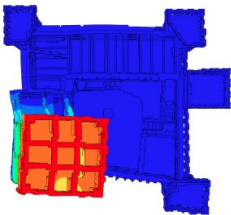
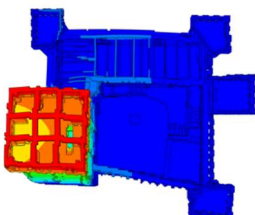
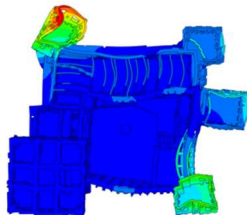
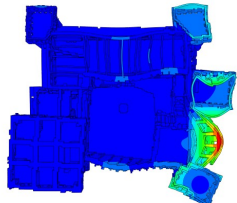
N-E tower	N tower		W body
			
Mode 4 (x+y)	Mode 6 (x+y)	Mode 8 (x+y)	Mode 3 (y)
Mastio	S-W tower		N-W tower
			
Mode 1 (x)	Mode 2 (y)	Mode 9 (x+y)	Mode 12 (x+y)

Table 4 Values of the participant mass fractions e^* obtained for each unit.

Unit	Modes (main direction)	Analysis	e^*	T [s]	M_x [%]	M_y [%]
Mastio (n. 4)	2 (y)	W	0.486	0.431	0.9	34
	2 (y)	E	0.559			
	1 (x)	S	0.554	0.47	32.4	0.9
	1 (x)	N	0.511			
N tower (n. 1)	6 (x+y)	E+S	0.529	0.216	3.9	2.6
	6 (x+y)	W+N	0.498			
	8 (x+y)	E+N	0.471	0.199	16.4	7.8
	8 (x+y)	W+S	0.521			
S-W tower (n. 3)	9 (x+y)	W+N	0.543	0.186	4.4	8.2
N-E tower (n.5)	4 (x+y)	W+N	0.618	0.251	6.1	1
W unit (n. 6)	3 (y)	E	0.174	0.284	0	8.1
	3 (y)	W	0.326			
N-W tower (n. 2)	12 (x+y)	E+N	0.555	0.162	1.5	6.8

For each unit, only the modes involving its dynamic response have been considered and, for each mode, the so obtained modal shapes have been fitted with exponential, polynomial and linear functions, which vary in plan and height.

Table 5 collects the main dynamic parameters of the first twelve modes in terms of period T and participant mass in the x and y directions computed referring to the mass of the whole structure (M_x and M_y , respectively). Furthermore, the main units activated by each mode are identified (the identification number of units refers to Fig. 13). It is worth noting that the modes of the Mastio (1 and 2 in Table 4) are coherent with the ones obtained from the dynamic identification [40], performed on the Mastio after the earthquake (equal to $T_{1,id}=0.581$ and $T_{2,id}=0.568$). A direct comparison of the numerical and experimental periods of the Mastio is not possible, since the first refers to an elastic condition while the second to a cracked one. However, computing the ratio T_1/T_2 with the experimental and numerical data, one can see that the results almost correspond ($T_1/T_2=1.09$ and $T_{1,id}/T_{2,id}=1.02$).

Table 5. Dynamic parameters of the first twelve modes.

Mode	T [s]	M_x [%]	M_y [%]	Involved units
1	0.47	32.4	0.9	4
2	0.431	0.9	34	4
3	0.284	0	8.1	6
4	0.251	6.1	1	5
5	0.227	0.3	6.8	4-5-9
6	0.216	3.9	2.6	1
7	0.209	0	0	1-7-9
8	0.199	16.4	7.8	1
9	0.186	4.4	8.2	3
10	0.182	0	0.5	1-3-5-7
11	0.166	4.5	3.8	2-3-6
12	0.162	1.5	6.8	2

Fig. 14 shows the modal shape in plan and a sketch with the 3D LPs applied in the pushover analyses for some units of the fortress. Table 6 collects the functions fitted from the modal shapes, showing the selected mode with its main direction (the axes are indicated in Fig. 13), the functions fitted from the maximum and minimum modal displacements assumed for the force distribution in the nonlinear pushover analyses (where z is the vertical axis), and the function and a sketch of the LP applied in plan. As one can see from the table, three kinds of LPs have been applied in plan (constant, parabolic and linear trapezoidal), with a vertical outline which varies in height. As it is possible to see from Fig. 14 and from Table 6, the applied distribution varies only in height while it remains constant in plan for some units (such as the Mastio), whereas for other units (such as the West unit), it varies both in height and in plan. More specifically, Table 6 collects: the kind of LP applied in plan (distinguishing between constant, parabolic and linear trapezoidal); the examined unit (Mastio, W unit, N-E tower, S-W tower, N-W tower, N tower); the selected modes with its main direction/directions; and the expressions of the functions used for the LP, fitted from the selected modal shapes. It has to be pointed

out that for those modes characterized by significant displacements both in the x and y directions (i.e. modes 4, 6, 8, 9 and 12), the pushover analyses have been performed by simultaneously applying the x and y component of the LP.

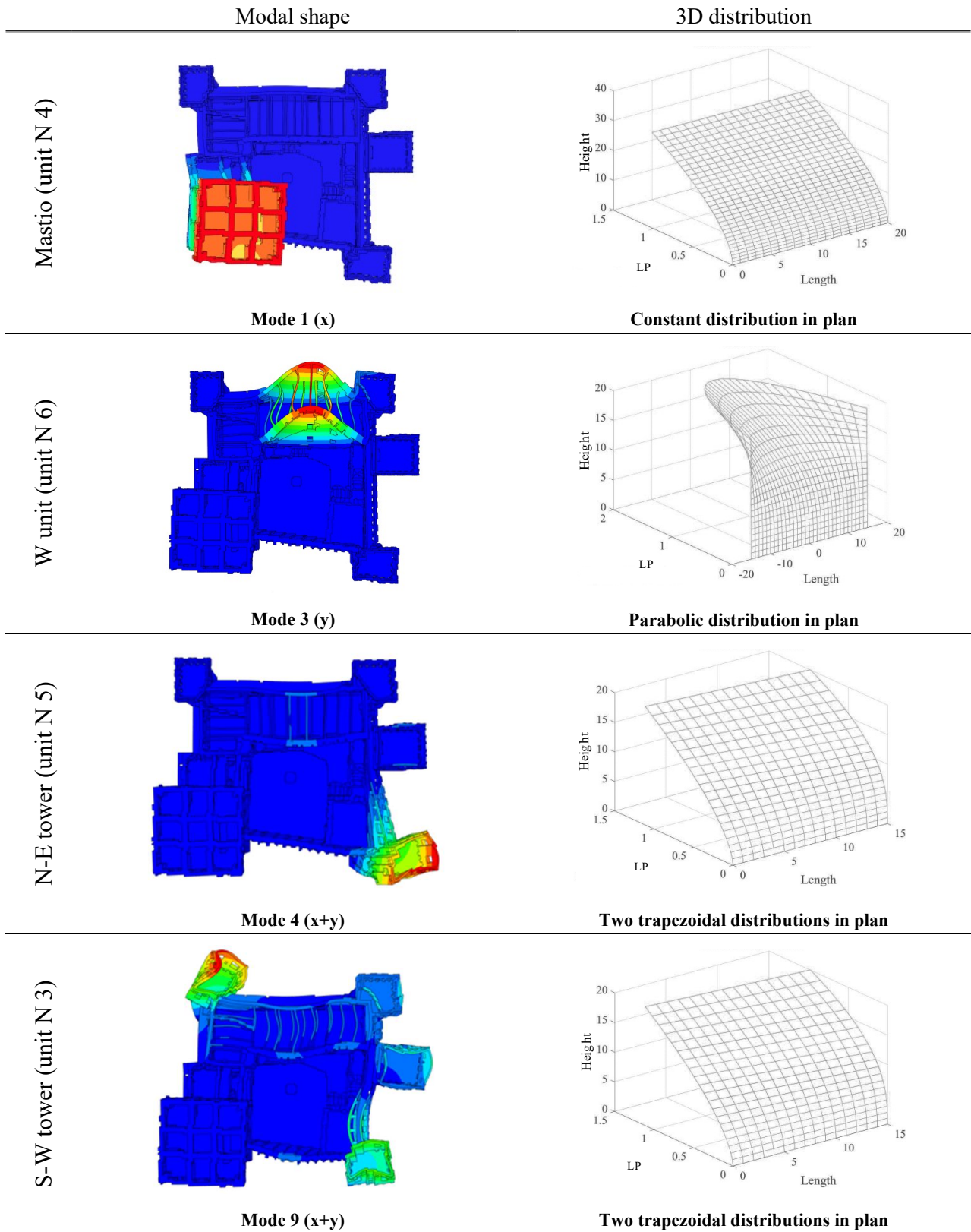


Fig. 14 - Examples of modal shapes and 3D LPs for different units.

Table 6. Functions of the LPs applied to the different units of the Fortress.

LP	Unit	Mode (dir.)	Function			
			Max	Min	Plan	
Constant	Mastio	1 (x dir)	$F(z) = 0.0021 \cdot z^{1.78}$	$F(z) = 0.0021z^{1.78}$	-	
		2 (y dir)	$F(z) = 0.0021 \cdot z^{1.77}$	$F(z) = 0.0021z^{1.77}$	-	
Parabolic	W unit	3 (y dir)	$F_1(z) = 4e^{-0.05} \cdot z^{3.54}$	$F_2(z) = 8e^{-0.05} \cdot z^{1.63}$	$F(x, z) = F_1(z) - \left(\frac{4x^2}{L^2} \cdot (F_1(z) - F_2(z)) \right)$	
		4 (x dir)	$F_1(z) = 0.0095 \cdot z^{1.59}$	$F_2(z) = 0.0003 \cdot z^{2.70}$	$F(x, z) = F_1(z) + \left(\frac{F_1(z) - F_2(z)}{L} \right) x$	
4 (y dir)	$F_1(z) = 0.01 \cdot z^{1.33}$	$F_2(z) = 5e^{-7} \cdot e^{0.70z}$				
9 (x dir)	$F_1(z) = 0.0124 \cdot z^{1.50}$	$F_2(z) = 0.0002 \cdot z^{2.72}$				
9 (y dir)	$F_1(z) = 0.01 \cdot z^{1.47}$	$F_2(z) = 0.0002 \cdot z^{2.56}$				
Linear trapezoidal on a and d	N-E tower	12 (x dir)	$F_1(z) = 0.0073z^{1.555}$	$F_2(z) = 0.0035e^{0.27z}$	$F(x, z) = F_1(z) + \left(\frac{F_1(z) - F_2(z)}{L} \right) x$	
		12 (y dir)	$F_1(z) = 0.0078z^{1.649}$	$F_2(z) = 0.0008z^{2.317}$		
Parabolic on a and b	N tower	6 (x dir)	$F_1(z) = 0.004 \cdot z^{1.76}$	$F_2(z) = 3e^{-5} \cdot z^{3.17}$		$F(x, z) = F_1(z) - \left(\frac{4x^2}{L^2} \cdot (F_1(z) - F_2(z)) \right)$
		6 (y dir)	$F_1(z) = 0.0063 \cdot z^{1.66}$	$F_2(z) = 0.0003 \cdot z^{2.42}$		
Parabolic on b and c	N tower	8 (-x dir)	$F_1(z) = 0.0079e^{0.26z}$	$F_2(z) = 0.0005z^{2.45}$	$F(x, z) = F_1(z) - \left(\frac{4x^2}{L^2} \cdot (F_1(z) - F_2(z)) \right)$	
		8 (y dir)	$F_1(z) = 0.0084e^{0.25z}$	$F_2(z) = 0.0007z^{2.15}$		

5.2 Nonlinear static analyses results

This section aims to describe how the results of the nonlinear static analyses in terms of pushover curves have been converted into the corresponding capacity curves of the equivalent SDOF systems. Once evaluated the LPs as explained in §5.1, the procedure has been firstly applied to the Mastio to verify its effectiveness. The aim of this example was to verify the reliability of applying the load pattern only to one unit of the building.

The results have been compared with those obtained by applying a unique load proportional to the height to the whole fortress; the latter is consistent with that usually proposed in codes [4, 49]. The results were compared in terms of damage pattern (Fig. 15), pushover curves (Fig. 16a) and capacity curves (Fig. 16b) showing a quite good agreement. Particularly, in order to make the two curves comparable, the base shear has been evaluated considering only the reaction forces of the nodes located at the base of the Mastio for both analyses. However, by applying a single LP that aims to excite contemporary the inertial forces on the whole fortress, only the nonlinear response of the Mastio (which is the first unit to be damaged) is activated (Fig. 15), while the response of the other minor towers is substantially still linear elastic. This is highlighted from the simulated damage pattern in Fig. 15a obtained by applying the force distribution to the whole fortress, where it is evident that the main damage is concentrated in the Mastio, while the other towers and the adjacent unit are interested only by a very light damage. Furthermore, in Fig. 16 the curves are rather akin in terms of stiffness and they differ of less than 10% in terms of maximum strength. It is also possible to observe that, when the LPs are applied to the whole fortress (black curves in Fig. 16), the softening effect is less pronounced.

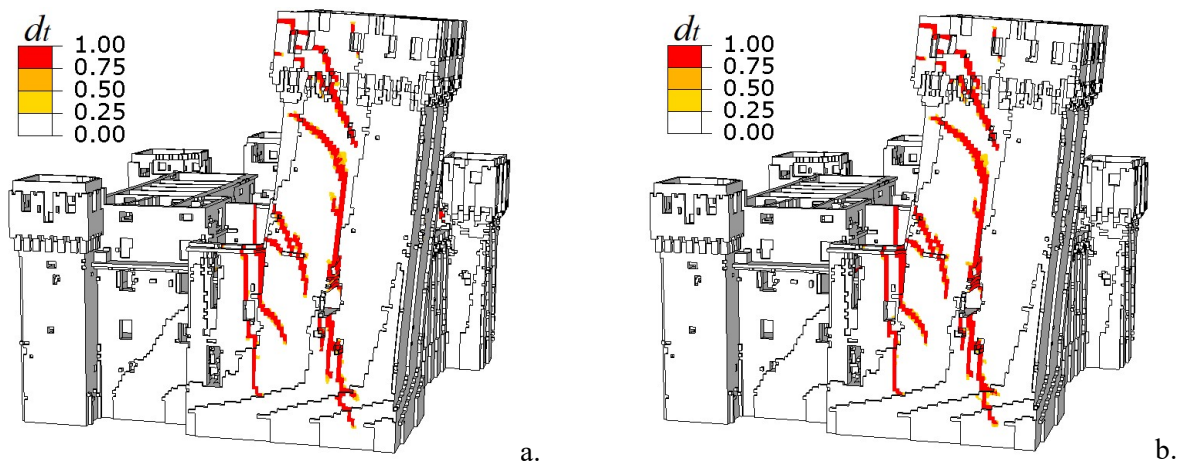


Fig. 15 - Comparison in terms of damage pattern obtained applying a unique LP to the whole fortress (a) and only to the Mastio (b).

In light of these results, the proposed procedure suggests to consider a global model of the whole fortress (to explicitly catch the interaction effects among units), and to push each unit with a specific LP fitted from the modal shapes. In this way, it is possible to describe the nonlinear behavior of all the units, including, for instance, the minor towers.

Dealing with masonry buildings, the pushover curves can be affected by the choice of the Control Node (CN), as discussed in [25]. However, in the specific case of fortified structures, this issue appears to be less relevant,

since the pushover analyses are performed on the global model, but with a load pattern only applied to a specific part (i.e. the Mastio tower under examination). Hence, the choice of the most proper CN would run out with the four edges of the tower (in plan), while in elevation, in order to explore the possible activation of mechanisms along the main body of each tower, it is necessary to define the CN at the highest parts.

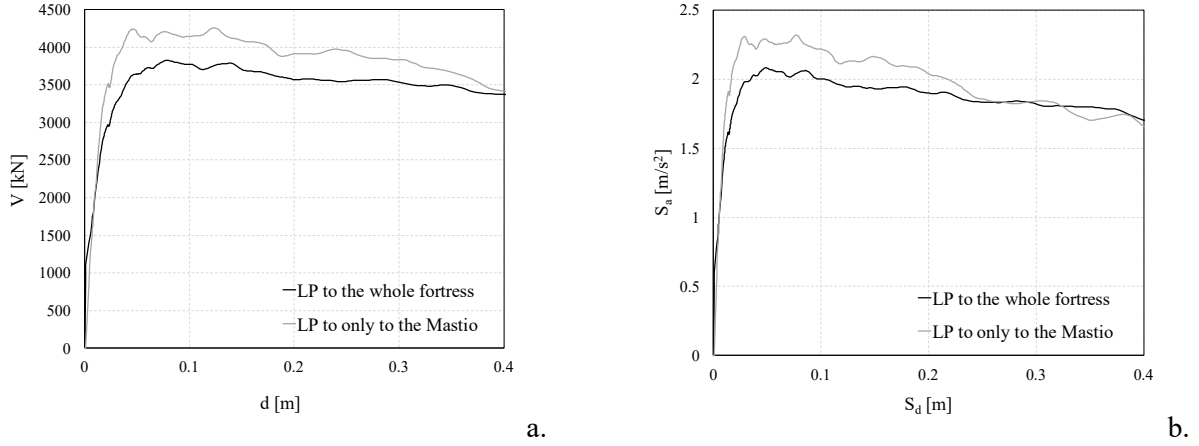


Fig. 16 – Comparison in terms of pushover curves (a) and capacity curves (b) obtained applying a unique LP to the whole fortress (graphs in black) and only to the Mastio (graphs in grey).

Nonlinear static analyses have been then carried out in both the directions +/- X e +/- Y, as indicated in Fig. 13. From the results, the following data have been extracted:

- the global shear at the base of the whole fortress, expressed as function of the average displacement at the top level of each unit;
- the displacements of several nodes evenly placed along the height of each unit at the beginning of the response, thus representative of an elastic phase. These values allowed calculating the participation coefficient and the participation mass necessary to transform the pushover curves into the capacity curves of the equivalent SDOF system.

Starting from these data, the pushover curves ($V-d$) of each unit have been obtained and then converted into the corresponding capacity curve (V^*-d^*), following the general principles of [33], adopted in [4] as well, and based on the evaluation of the participation coefficient Γ and the mass M^* of each unit (see Eq. (4), where ϕ_i is the i^{th} component of the eigenvector representative of the first modal shape and m_i is the correspondent modal mass). Hence, the capacity curve was obtained by dividing the displacement d by Γ ($d^*=d/\Gamma$) and the base shear by the product ΓM^* ($V^*=V/(\Gamma M^*)$), where Γ and M^* were related to the unit under investigation.

$$\Gamma = \frac{\sum m_i \phi_i}{\sum m_i \phi_i^2} = \frac{\sum m_i \phi_i}{\sum m_i \phi_i^2} \quad (4)$$

6 Validation of the proposed procedure

This section presents the results of the application of the proposed procedure to the examined case study, in terms of comparison between the seismic demand and the system capacity. In particular, in this case, the seismic demand came from the records of the SAN0 station from the ITACA network, which was very near to the Fortress. Two seismic shocks of comparable entity occurred in May 2012. However, no near-field records of the first shock were available. Hence, in the examined case, the actual record that hit the monument on the 29th May 2012 was considered as seismic action.

Fig. 17 shows: a) the localization of the SAN0 station with respect to the Fortress; b) the comparison in terms of acceleration-displacement response spectra of the two components North-South (NS) and East-West (EW) of the actual record of the 29th May 2012.

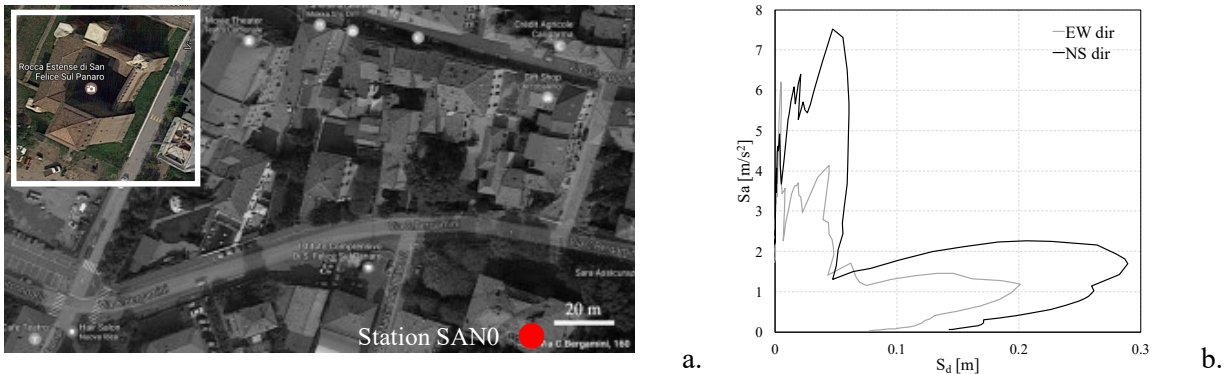


Fig. 17 – a) Localization of the SAN0 station; b) Comparison in terms of acceleration-displacement response spectra between the NS and the EW components of the actual 29th May 2012 seismic event (from SAN0 station - ITACA network).

The results were interpreted in terms of expected ductility demand μ_{pp} , representative of the ductility reached by the different units during the 2012 earthquake. This parameter has been assumed as reference to estimate the entity of the damage level attained together with its qualitative comparison with the actual one occurred. Indeed, it is expected that the units with higher values of ductility demand would correspond to the ones characterized by a more significant damage (in terms of spread and gravity of the cracks).

6.1 Assessment of the expected seismic demand

The first step to evaluate the ductility demand was the estimation of the seismic demand d_{pp} expected from the 2012 earthquake. This latter was evaluated by applying the Capacity Spectrum Method (CSM) [34], since recent studies proved that other methods of verification proposed in literature and in Standards (as the N2 method [33]) cannot be considered equally reliable for masonry structures, such as the examined one [27, 28, 35].

The CSM is based on the use of overdamped reduced spectra, computed using a reduction coefficient (ξ) aimed to conventionally take into account the progressive nonlinear response through the concept of hysteretic

damping for ductility values higher than 1. In the examined case, the overdamped response spectrum has been evaluated on the basis of the well-known reduction law, adopted in [4] and [5] as well:

$$\xi = \xi_{el} + \xi_{max} \left(1 - \frac{1}{\mu^\beta}\right) \quad (5)$$

where ξ_{el} is the elastic damping (assumed equal to 5%); ξ_{max} is the maximum hysteretic damping (assumed equal to 20%); μ is the ductility computed starting from the displacement associated to the considered limit state, calculated once converted the capacity curve in the equivalent bi-linear; β is a coefficient herein assumed equal to 0.6. The latter value is compatible with the ones traditionally assumed for masonry structures [56, 57]. It is worth noting that the evaluation of the bi-linear curve from the capacity curve is not strictly necessary to apply the CSM but only to evaluate the ductility μ .

Therefore, once evaluated the capacity curve for each unit, the expected seismic demand d_{PP} was evaluated as the spectral displacement obtained comparing the capacity curve with the overdamped response spectrum generated from the actual records of May 2012.

Fig. 18 shows, by way of example in the case of the Mastio, the comparison between the capacity curve of the system (in black) – obtained as illustrated in §5.2 – and the actual overdamped spectrum (through the continuous grey). In this case, the response spectrum has been obtained from the EW component of the actual record (grey dotted line in the figure), properly overdamped as above described, in order to consider the progressive nonlinear response of the system for ductility values higher than 1.

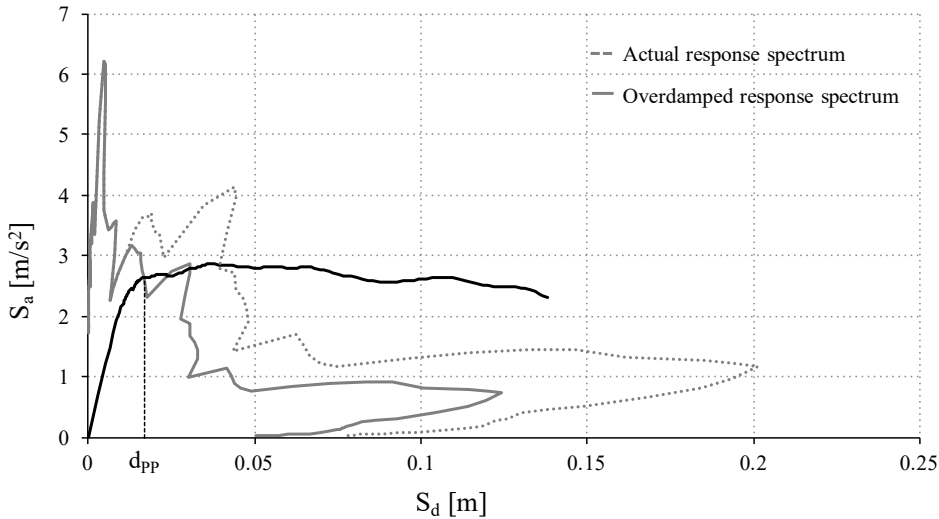


Fig. 18 – Comparison between the capacity curve of the system and the actual overdamped spectrum (EW component of the record) for the estimation of the expected seismic demand.

Although the use of a real response spectrum can be conventional in the application of the CSM (due to its irregular shape), it has been considered more representative with the aim of validation being more representative to the real event that hit the structure.

It has to be pointed out that, in the CSM method framework, the seismic assessment has been developed:

- in the X and Y directions for the units where the LP applied in the pushover analyses pushed the unit in those directions one at a time;
- with respect to the resultant axis of the two forces distributions applied simultaneously along the orthogonal axes X and Y. In this case, the values of shear and displacement obtained from each pushover have been projected with respect to the above-mentioned axes.

6.2 Definition of the ductility demand and comparison with the actual damage

Once evaluated the demand displacement d_{PP} , it was necessary to estimate a conventional yielding point d_y to convert d_{PP} into the expected ductility demand to provide an estimate of the comparison with the actual damage level occurred. To this aim, a bi-linear curve was defined according to the principles proposed for masonry structures by [33] and assuming an initial stiffness which was representative of the actual one of each unit.

Then, the actual ductility demand μ_{PP} is computed as $\mu_{PP} = \frac{d_{PP}}{d_y}$ for $d_{PP} > d_y$ (i.e. when it is higher than 1).

Table 7 presents a summary of the results obtained for all the units (identified by the numbers of Fig. 13), in terms of:

- period which defines the initial elastic branch of the bi-linear curve (T^*);
- value of the calculated ductility demand μ_{PP} , obtained alternatively comparing the capacity curve of each unit with the overdamped response spectrum obtained from the NS or the EW component of the actual record;
- direction of the analysis, i.e. the cardinal point towards which the LP pushes the unit.

Moreover, an empirical Damage level graduated according to the EMS98 scale [58] has been assigned to each unit, distinguishing between the one occurred in the main body of the unit (D) and the one interesting the tower top parts (\bar{D}). In particular, concerning the assignment of D, the criteria summarized in Table 8 have been adopted, while for the top parts (\bar{D}) the damage level has been assigned depending on the seriousness and extent of the damage interesting the towers corbels, battlements and roofs. The qualitative correspondence between the obtained ductility level μ_{PP} and the empirical damage level assigned has been assumed as further factor for assessing the reliability of the numerical analysis performed. In fact, values of μ_{PP} higher than 1 indicated the structural response progressed in the nonlinear field and increasing values should be associated to more significant and spread damage.

Table 7. Results of the proposed procedure validation.

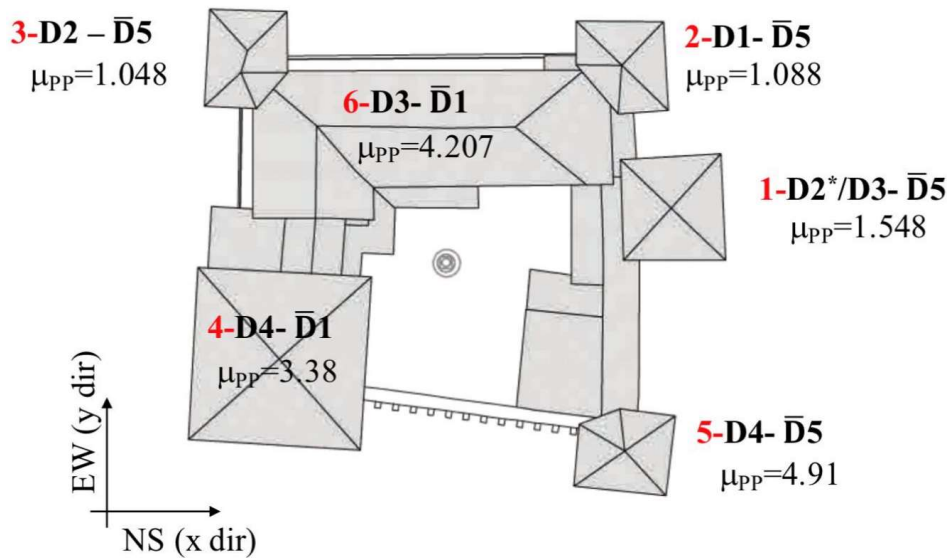
Unit	N	Dir.	T*[s]	μ_{PP} [-]	μ_{PP} [-]
				(NS record)	(EW record)
Mastio	4	W	0.379	3.373	1.192
		S	0.471	3.229	2.397
		E	0.466	3.306	2.484
		N	0.419	3.383	1.417
North tower	1	E+S	0.120	0.768	0.831
		W+N	0.176	1.312	1.309
		E+N	0.219	1.409	1.159
		W+S	0.0844	1.548	1.172
S-W tower	3	W+N	0.182	1.046	1.048
N-E tower	5	W+N	0.306	4.911	0.957
N-W tower	2	E+N	0.127	1.088	0.674
West unit	6	W	0.518	4.207	3.843
		E	0.509	3.590	3.253

Fig. 19 indicates, on the Fortress plan, the damage levels (D and \bar{D}) associated to each unit and the maximum ductility demands obtained from the adopted procedure. The number in red identifies the different units (as in Fig. 13). As one can see from Fig. 19, it is clear that referring to the damage in the top parts (\bar{D}), damage mechanisms due to the interactions with the roof are present in almost all towers (sometimes the roofs even collapsed). Instead, the damage interesting the tower main body is more differentiated. In particular, from the observation of the post-earthquake damage (confirmed also by the damage pattern numerically simulated), it appears that two different situations occurred:

- a) the damage occurs first in the top parts; hence, the forces in the pushover are not able to further increase and the tower main body is not damaged, remaining almost in the elastic phase. This for example happened in N-W and S-W towers (respectively, units 2 and 3 in Fig. 13);
- b) the damage occurs first in the tower main body and then it spreads across the top parts. This latter happened in the Mastio, the N-E tower and the N tower (units 4, 5 and 1 respectively in Fig. 13).

Interpreting the results in light of these two possible occurred situations, one can observe that there is a good correspondence between the level of damage and the highest value of maximum expected ductility demand

μ_{PP} . In fact, the first condition (a) is associated to low values of ductility (N-W and S-W towers reach a maximum ductility level equal to 1.088 and 1.048, respectively), instead the second one (b) corresponds to higher level of expected ductility. This latter is for example the case of the North tower (with a maximum ductility level in the most punitive direction equal to 1.548), of the N-E tower (with a maximum ductility equal to 4.911) and of the Mastio (with maximum ductility level in the most punitive direction equal to 3.383).



* After the first seismic shock

Fig. 19 – Damage levels associated to towers' main body (D) and top parts (\bar{D}) and maximum obtained ductility demands, identified on the Fortress' plan.

Table 8. Criteria for the definition of the damage level D ([58]) expressed in Fig. 19.

Damage Level	Observed damage
D2	Visible cracks. However, the structure preserves its structural functionality but is close to the attainment of its maximum shear strength
D3	Significant and spread cracks. The structure has reached the maximum resistance to horizontal actions and present permanent deformations
D4	Partial local collapse, due to the in-plane behavior of the units
D5	The unit is near to the collapse

Furthermore, the comparison with the actual damage occurred after the 2012 earthquake highlighted a very good correspondence with the one numerically simulated. Hence, the obtained results confirmed the proposed procedure reliability. Fig. 20 and Fig. 21 show the damage contour plots in terms of tensile damage (d_t), extracted at the maximum expected ductility demand (performance points), for some units of the fortress. For the sake of comparison, photos of the actual crack pattern experienced by the structure due to the 2012 Emilia earthquake are reported as well. A very good agreement between the simulated crack pattern and the actual one is observed in terms of both damage level and crack location.

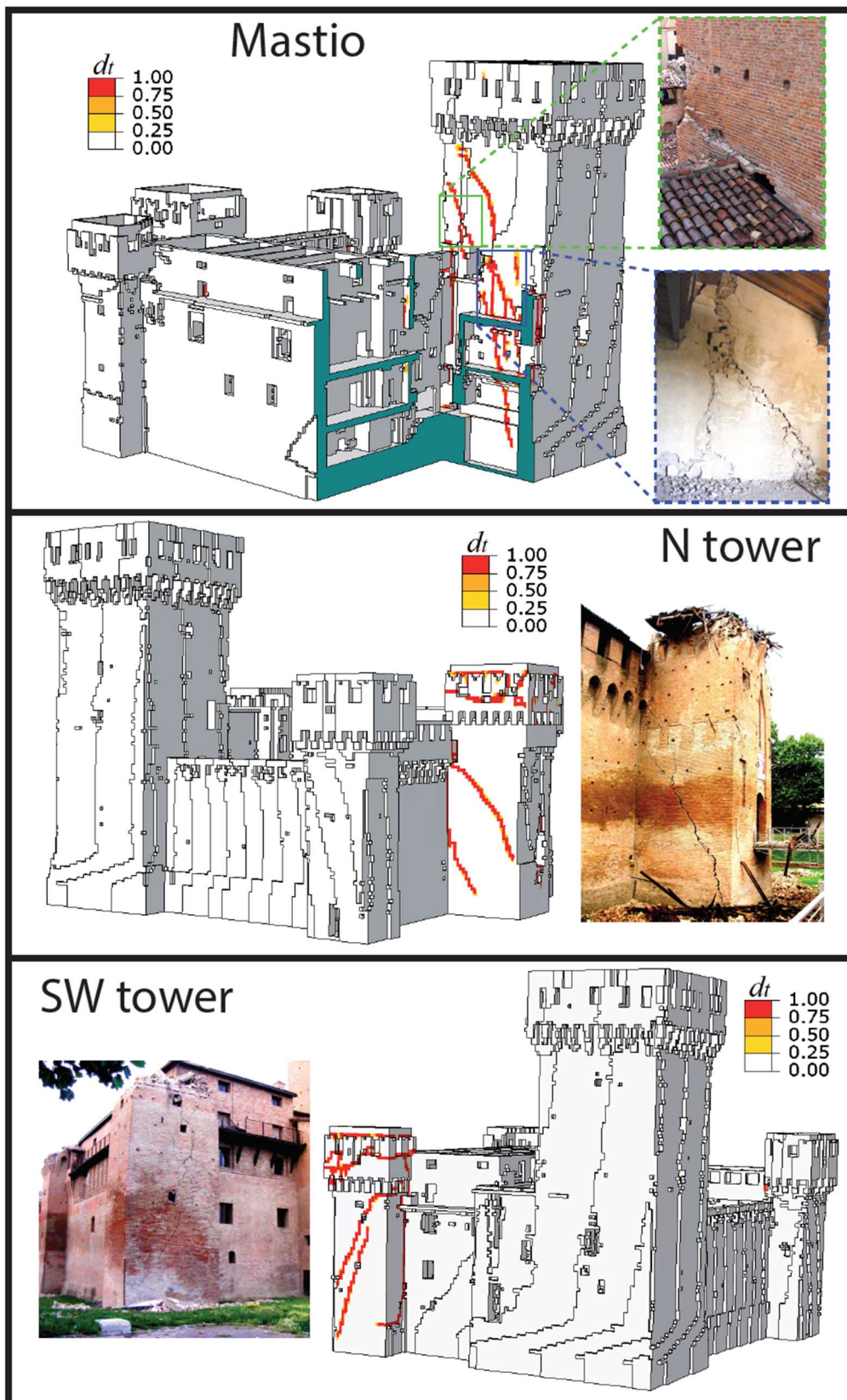


Fig. 20 - Comparison between the actual damage pattern and the simulated one for some units of the fortress at the performance point: Mastio (S dir.), N tower (W+S dir.) and SW tower (W+N dir.).

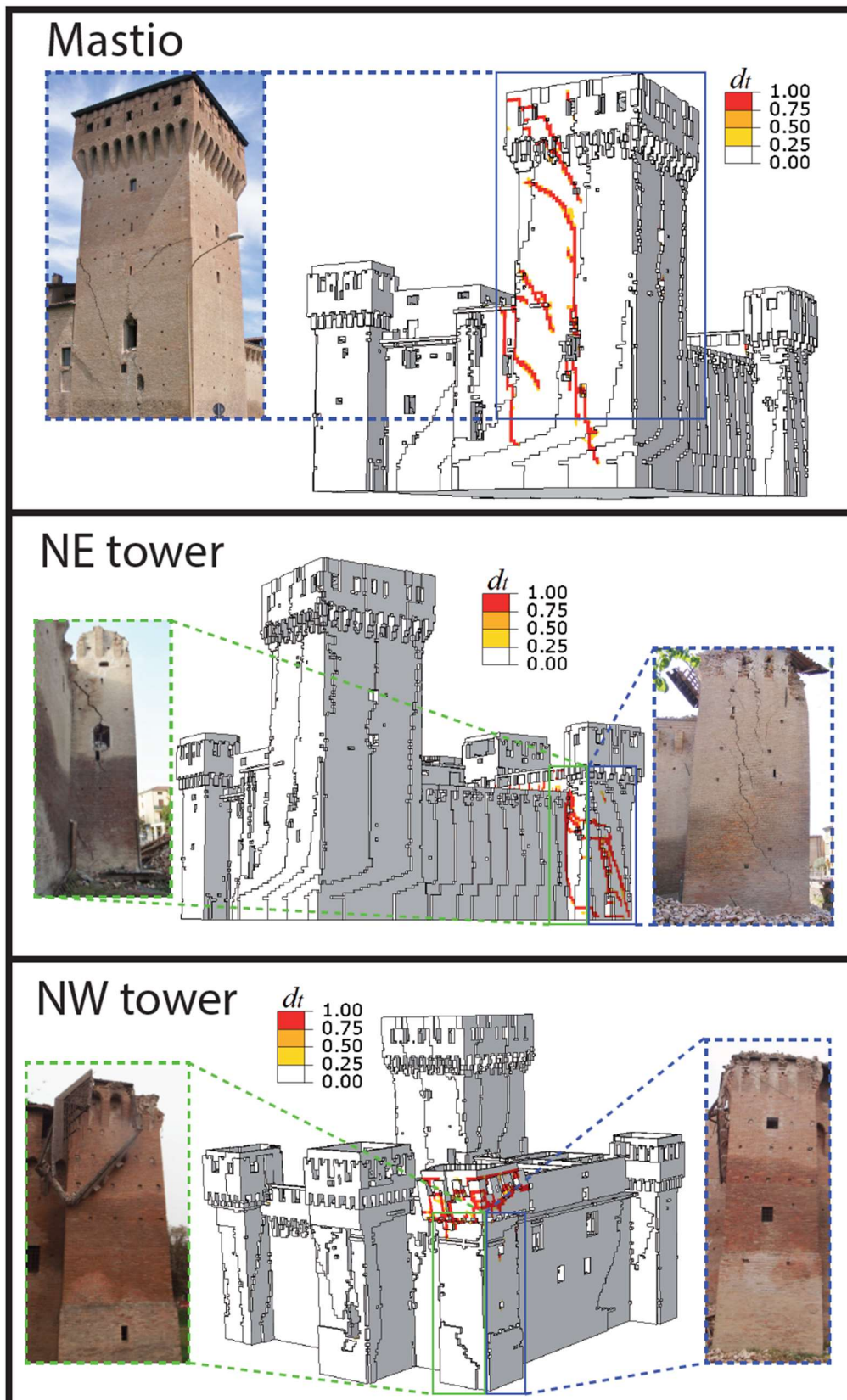


Fig. 21 - Comparison between the actual damage pattern and the simulated one for some units of the fortress at the performance point: Mastio (E dir.), NE tower (W+N dir.) and NW tower (E+N dir.).

Finally, it has to be pointed out that, although only the modes related to the minor towers (non-uniformly constrained at the curtain walls) presented significant torsion, the load patterns assumed for these towers were

not purely torsional, but rather a coupling of bending and torsional loads, given the two trapezoidal distributions in plan and the exponential law in height. This approach provides realistic results, as the critical comparison between the computed damage pattern and the actual one experienced by the structure during the Emilia earthquake (2012) appears in good agreement. Indeed, concerning for example the SW tower, there was no way to reproduce the pseudo vertical crack in the photo of Fig. 20 with the standard load patterns (uniform or triangular distributions) of pushover analysis.

7 Conclusions

The seismic assessment of interacting structural units in complex historic masonry constructions is a very difficult task, not manageable *a priori* through well-defined procedures of analysis and verification. As a first attempt to provide operative tools, this paper proposed a procedure for the seismic assessment of such complex structures.

The procedure requires: a numerical model of the entire aggregation of units, in order to explicitly consider the interaction effects among these latter; the execution of a modal analysis to define the modes involving the dynamic response of each units and their modal shapes; the execution of a series of pushover analyses (one for each unit) by applying the load pattern fitted according to the identified modal shapes; the conversion of the pushover curve of each unit into the corresponding capacity curve of the equivalent SDOF system, in order to perform the seismic verification.

The procedure has been then applied to a case-study, the medieval fortress in San Felice sul Panaro, significantly damaged by the 2012 Emilia earthquake. The results are good in terms of comparison between the damage experienced by the structure and the one predicted, showing the potential of the proposed procedure. Although in the analysed case the predictions were facilitated as the building already exhibited an earthquake damage, the proposed procedure must be, in general, applied carefully in order to limit the analyst's interpretation. To this aim, the analysis of the historical transformations, the investigation of the constructive features and the examination of the occurred damage in similar structures can address the analyst in the proper identification of the seismic response, providing in this way reliable results.

Finally, the procedure proposed in this paper appears general and potentially applicable also in conjunction to other numerical modelling strategies and other types of monumental buildings. Indeed, as the generated FE mesh could be imported in other codes, it could be used in other computational analysis frameworks (e.g. DEM, micro-models, multi-scale models, FE limit analysis, etc.). Additionally, the extendibility of the proposed procedure to other historical building typologies, which appears preliminary affordable, could represent an interesting future scientific development.

ACKNOWLEDGEMENTS

The Authors would like to thank the municipality of San Felice sul Panaro, ABACUS (www.arcoabacus.it) for the supply of the fortress laser scanner survey and CINECA (www.cineca.it) for the hardware resources.

Financial support by the Italian Ministry of Education, Universities and Research MIUR is gratefully acknowledged (PRIN2015 “Advanced mechanical modeling of new materials and structures for the solution of 2020 Horizon challenges” prot. 2015JW9NJT_018).

REFERENCES

- [1] S. Cattari, S. Degli Abbatì, D. Ferretti, S. Lagomarsino, D. Ottonelli and A. Tralli, “Damage assessment of fortresses after the 2012 Emilia earthquake (Italy),” *Bulletin of Earthquake Engineering*, vol. 12, no. 5, pp. 2333–2365, 2014 doi:10.1007/s10518-013-9520-x.
- [2] E. Coisson, D. Ferretti and E. Lenticchia, “Analysis of damage mechanisms suffered by Italian fortified buildings hit by earthquakes in the last 40 years,” *Bulletin of Earthquake Engineering*, vol. 15, no. 12, p. 5139–5166, 2017 doi:10.1007/s10518-017-0172-0.
- [3] V. Sarhosis, G. Milani, A. Formisano and F. Fabbrocino, “Evaluation of different approaches for the estimation of the seismic vulnerability of masonry towers,” *Bulletin of Earthquake Engineering*, vol. 16, no. 3, p. 1511–1545, 2017.
- [4] *EN 1998-3. Eurocode 8: design of structures for earthquake resistance-part 3: assessment and retrofitting of buildings. CEN (European Committee for Standardization), Brussels, Belgium; 2005..*
- [5] *DPCM 9/2/2011. Linee guida per la valutazione e la riduzione del rischio sismico del patrimonio culturale con riferimento alle Norme tecniche delle costruzioni di cui al decreto del Ministero delle Infrastrutture e dei trasporti del 14 gennaio 2008.*
- [6] G. Castellazzi, A. M. D’Altri, G. Bitelli, I. Selvaggi and A. Lambertini, “From Laser Scanning to Finite Element Analysis of Complex Buildings by Using a Semi-Automatic Procedure,” *Sensors*, vol. 15, no. 8, p. 18360–18380, 2015 doi:10.3390/s150818360.
- [7] G. Castellazzi, A. M. D’Altri, S. de Miranda and F. Ubertini, “An Innovative Numerical Modeling Strategy for the Structural Analysis of Historical Monumental Buildings,” *Engineering Structures*, vol. 132, p. 229–248, 2017 doi:10.1016/j.engstruct.2016.11.032.
- [8] S. Tiberti, M. Acito and G. Milani, “Comprehensive FE Numerical Insight into Finale Emilia Castle Behavior Under 2012 Emilia Romagna Seismic Sequence: Damage Causes and Seismic Vulnerability Mitigation Hypothesis,” *Engineering Structures*, vol. 117, p. 397–421, 2016 doi:10.1016/j.engstruct.2016.02.048.

- [9] G. Milani, M. Valente and C. Alessandri, “The Narthex of the Church of the Nativity in Bethlehem: A Non-Linear Finite Element Approach to Predict the Structural Damage,” *Computers & Structures*, 2017 doi:10.1016/j.compstruc.2017.03.010.
- [10] M. Betti, M. Orlando and A. Vignoli, “Static behaviour of an Italian Medieval Castle: Damage assessment by numerical modelling,” *Computers & Structures*, vol. 89, no. 21-22, p. 1956–1970, 2011 doi:10.1016/j.compstruc.2011.05.022.
- [11] G. Milani, R. Shehu and M. Valente, “Role of Inclination in the Seismic Vulnerability of Bell Towers: FE Models and Simplified Approaches,” *Bulletin of Earthquake Engineering*, vol. 15, no. 4, p. 1707–1737, 2016 doi:10.1007/s10518-016-0043-0.
- [12] M. Acito, M. Bocciarelli, C. Chesi and G. Milani, “Collapse of the clock tower in Finale Emilia after the May 2012 Emilia Romagna earthquake sequence: Numerical insight,” *Engineering Structures*, vol. 72, pp. 70-91, 2014.
- [13] M. Valente and G. Milani, “Non-linear dynamic and static analyses on eight historical masonry towers in the North-East of Italy,” *Engineering Structures*, vol. 114, p. 241–270, 2016.
- [14] M. Valente and G. Milani, “Seismic assessment of historical masonry towers by means of simplified approaches and standard FEM,” *Construction and Building Materials*, vol. 108, p. 74–104, 2016.
- [15] M. Acito, C. Chesi, G. Milani and S. Torri, “Collapse analysis of the Clock and Fortified towers of Finale Emilia, Italy, after the 2012 Emilia Romagna seismic sequence: Lesson learned and reconstruction hypotheses,” *Construction and Building Materials*, vol. 115, pp. 193-213, 2016.
- [16] A. Formisano and A. Marzo, “Simplified and Refined Methods for Seismic Vulnerability Assessment and Retrofitting of an Italian Cultural Heritage Masonry Building,” *Computers & Structures*, vol. 180, p. 13–26, 2017.
- [17] R. Marques and P. B. Lourenço, “Possibilities and comparison of structural component models for the seismic assessment of modern unreinforced masonry buildings,” *Computers & Structures*, vol. 89, no. 21-22, p. 2079–2091, 2011 doi:10.1016/j.compstruc.2011.05.021.
- [18] G. Castellazzi, A. M. D’Altri, S. de Miranda, F. Ubertini, G. Bitelli, A. Lambertini, I. Selvaggi and A. Tralli, “A mesh generation method for historical monumental buildings: An innovative approach,” in

Proceedings of the VII European Congress on Computational Methods in Applied Sciences and Engineering (ECCOMAS Congress 2016), Crete Island, 2016 doi:10.7712/100016.1823.11948.

- [19] A. M. D'Altri, G. Milani, S. de Miranda, G. Castellazzi and V. Sarhosis, "Stability analysis of leaning historic masonry structures," *Automation in Construction*, vol. 92, pp. 199-213, 2018.
- [20] M. Korumaz, M. Betti, A. Conti, G. Tucci, G. Bartoli, V. Bonora, A. G. Korumaz and L. Fiorini, "An integrated Terrestrial Laser Scanner (TLS), Deviation Analysis (DA) and Finite Element (FE) approach for health assessment of historical structures. A minaret case study," *Engineering Structures*, vol. 153, p. 224–238, 2017 doi:10.1016/j.engstruct.2017.10.026.
- [21] G. Castellazzi, A. M. D'Altri, S. de Miranda, A. Chiozzi and A. Tralli, "Numerical Insights on the Seismic Behavior of a Non-Isolated Historical Masonry Tower," *Bulletin of Earthquake Engineering*, vol. 16, no. 2, p. 933–961, 2018 doi.org/10.1007/s10518-017-0231-6.
- [22] S. Lu, K. Beyer, V. Bosiljkov, C. Butenweg, D. D'Ayala, D. Degee, K. J. M. Gams, S. Lagomarsino, A. Penna, N. Mojsilovic, F. Da Porto, L. Sorrentino and E. Vintzileo, "Amendment of masonry chapter of Eurocode 8," in *6th World Conference on Earthquake Engineering*, Santiago, Chile, 2017.
- [23] A. Mouyiannou, M. Rota, A. Penna and G. Magenes, "Identification of suitable limit states from nonlinear dynamic analyses of masonry structures," *Journal of Earthquake Engineering*, vol. 18, no. 2, pp. 231-263, 2014.
- [24] A. Galasco, S. Lagomarsino and A. Penna, "On the use of pushover analysis for existing masonry buildings," in *First European conference on earthquake engineering and seismology*, Geneva, Switzerland, 2006.
- [25] S. Lagomarsino and S. Cattari, "Seismic Performance of Historical Masonry Structures Through Pushover and Nonlinear Dynamic Analyses," in *Perspectives on European Earthquake Engineering and Seismology*, Istanbul, Turkey, 2015.
- [26] S. Lagomarsino and S. Cattari, "PERPETUATE guidelines for seismic performance-based assessment of cultural heritage masonry structures," *Bulletin of Earthquake Engineering*, vol. 13, no. 1, p. 13–47, 2014.
- [27] S. Marino, *Nonlinear static procedures for the seismic assessment of irregular URM buildings*, Genoa: PhD Dissertation, University of Genoa, 2018.

- [28] S. Marino, S. Cattari and S. Lagomarsino, “Use of nonlinear static procedures for irregular URM building in literature and codes,” in *16th European Conference on Earthquake Engineering*, Thessaloniki, Greece, 2018.
- [29] P. Fajfar, “Analysis in seismic provisions for buildings: past, present and future,” *Bulletin of Earthquake Engineering*, 2017 (in press) doi:10.1007/s10518-017-0290-8.
- [30] F. Minghini, E. Bertolesi, A. Del Grosso, G. Milani and A. Tralli, “Modal pushover and response history analyses of a masonry chimney before and after shortening,” *Engineering Structures*, vol. 110, p. 307–324, 2016.
- [31] A. Galasco, S. Lagomarsino and A. Penna, “On the use of pushover analysis for existing masonry buildings,” in *First European Conference on Earthquake Engineering*, Geneva, Switzerland, 2006.
- [32] *ASCE/SEI 41-13, Seismic Evaluation and Retrofit of Existing Buildings*, Reston, Virginia, 2014.
- [33] P. Fajfar, “Capacity spectrum method based on inelastic demand spectra,” *Earthquake Engineering and Structural Dynamics*, vol. 28, no. 9, p. 979–993, 1999.
- [34] S. A. Freeman, “The capacity spectrum method as a tool for seismic design,” in *11th European Conference of Earthquake Engineering*, Paris, France, 1998.
- [35] G. Guerrini, F. Graziotti, A. Penna and G. Magenes, “Improved evaluation of inelastic displacement demands for short-period masonry structures,” *Earthquake Engineering & Structural Dynamics*, vol. 46, no. 9, p. 1411–1430, 2017.
- [36] C. Calderini, S. Cattari, S. Degli Abbatì, S. Lagomarsino, D. Ottonelli and M. Rossi, “Modelling strategies for seismic global response of building and local mechanisms. PERPETUATE (EU-FP7 Research Project), Deliverable D26 (www.perpetuate.eu/D26/),” 2012.
- [37] V. Sarhosis, K. Bagi, J. Lemos and G. Milani, *Computational modeling of masonry structures using the discrete element method*, USA: IGI Global, 2016.
- [38] V. Gulinelli, *Il castello di San Felice sul Panaro e le fosse del castello: da ricerche d'archivio, notizie urbanistiche, storiche e di cronaca*, S. G. Persiceto, Li.Pe., 1994.

- [39] G. Bitelli, G. Castellazzi, A. M. D'Altri, S. de Miranda, A. Lambertini and I. Selvaggi, "On the generation of numerical models from point clouds for the analysis of damaged Cultural Heritage," in *Florence HeriTech, The Future of Heritage Science and Technologies*, Florence, Italy, 2018.
- [40] E. Bassoli, L. Vincenzi, A. M. D'Altri, S. de Miranda, M. Forghieri and C. G., "Ambient vibration-based finite element model updating of an earthquake-damaged masonry tower," *Structural Control and Health Monitoring*, 2018 doi.org/10.1002/stc.2150.
- [41] S. Casolo, V. Diana and G. Uva, "Influence of soil deformability on the seismic response of a masonry tower," *Bulletin of Earthquake Engineering*, vol. 15, no. 5, p. 1991–2014, 2016.
- [42] F. De Silva, F. Ceroni, S. Sica and F. Silvestri, "Non-linear analysis of the Carmine bell tower under seismic actions accounting for soil–foundation–structure interaction," *Bulletin of Earthquake Engineering (in press)*, 2017 doi:10.1007/s10518-017-0298-0.
- [43] A. W. Page, "The biaxial compressive strength of brick masonry," in *Proceedings of the Institution of Civil Engineers*, 1981.
- [44] P. B. Lourenço and J. G. Rots, "Multisurface Interface Model for Analysis of Masonry Structures," *Journal of Engineering Mechanics*, vol. 123, no. 7, p. 660–668, 1997.
- [45] L. Berto, A. Saetta, R. Scotta and R. Vitaliani, "An Orthotropic Damage Model for Masonry Structures," *International Journal for Numerical Methods in Engineering*, vol. 55, no. 2, p. 127–157, 2002.
- [46] A. M. D'Altri, G. Castellazzi, S. de Miranda and A. Tralli, "Seismic-Induced Damage in Historical Masonry Vaults: A Case-Study in the 2012 Emilia Earthquake-Stricken Area," *Journal of Building Engineering*, vol. 13, p. 224–243, 2017 doi:10.1016/j.job.2017.08.005.
- [47] J. Lee and G. L. Fenves, "Plastic-Damage Model for Cyclic Loading of Concrete Structures," *Journal of Engineering Mechanics*, vol. 124, no. 8, p. 892–900, 1998 doi:10.1061/(asce)0733-9399(1998)124:8(892).
- [48] R. van der Pluijm, "Shear behaviour of bed joints," in *6th North American Masonry Conference, 6-9 June 1993*, Philadelphia, Pennsylvania, USA, 1993.
- [49] *DM 14/01/2008. Nuove norme tecniche per le costruzioni. Ministero delle Infrastrutture (GU n.29 04/02/2008), Rome, Italy [New technical norms on constructions].*

- [50] *Circolare 617-02/02/2009. Istruzioni per l'applicazione delle nuove norme tecniche per le costruzioni di cui al decreto ministeriale 14 Gennaio 2008 [Instructions for the application of the new technical norms on constructions].*
- [51] G. Fortunato, M. F. Funari and P. Lonetti, "Survey and seismic vulnerability assessment of the Baptistery of San Giovanni in Tumba (Italy)," *Journal of Cultural Heritage*, vol. 26, pp. 64-78, 2017.
- [52] S. Casolo and G. Milani, "Simplified out-of-plane modelling of three-leaf masonry walls accounting for the material texture," *Construction and Building Materials*, vol. 40, p. 330–351, 2013.
- [53] V. Turnšek and F. Čačovič, "Some experimental results on the strength of brick masonry walls," in *2nd International Brick Masonry Conference*, 1971.
- [54] V. Turnšek and P. Sheppard, "The shear and flexural resistance of masonry walls," in *International Research Conference on Earthquake engineering*, Skopje, Japan, 1980.
- [55] *Abaqus®. Theory manual, version 6.14, 2014.*
- [56] S. Cattari and S. Lagomarsino, "Masonry structures," in *Developments in the field of displacement based seismic assessment*, IUSS Press (PAVIA) and EUCENTRE, 2013, pp. 151-200.
- [57] C. Blandon and M. Priestley, "Equivalent viscous damping equations for direct displacement based design," *Journal of Earthquake Engineering*, vol. 9, no. 2, pp. 257-278, 2005.
- [58] G. Grunthal, "European Macroseismic Scale," *Centre Européen de Géodynamique et de Séismologie*, vol. 15, 1998.